LISE++

version 6.4

Contents:

1. LISE for "unprivileged" users

The program "LISE" was initially developed for Personal Computer (PC) under DOS, and then Windows 95 and 98. With these systems, the user of PC was the absolute owner of the computer. Nowadays the multitask operational systems Windows 2000 & XP are installed on the majority of PCs. LISE++ is mostly used in laboratories, where PC users usually have no administrative privileges, and the following problems are encountered:

- It is impossible to load the program under WinXP because the file "*lise.dbf*" is set to read-only by the system;
- It is forbidden to save LISE user files in the directory "Program files\LISE\files", as well as to keep user settings of the code;
- The programs "Charge", "PACE4", and "BI" can not be loaded because it is impossible to open temporary files in the directory "Program files\LISE".

All of the above-mentioned problems were solved in the new version. However the possibility to install the code without administrative privileges in a user directory (creating a temporary directory for unzipped files) has been removed.

1.1. The "\user\MyDocuments\LISE" directory

What happens now, when the user loads the program, after it has been installed by the administrator? The program tries to open the file "*lise.ini*" for writing. If the attempt is unsuccessful, the user is automatically considered without privileges, and the program uses the directory "\user\MyDocuments\LISE" as LISE's working directory. If this directory is missing, the code will create the directory "LISE" and subdirectories "files", "config", "bin", "options" etc. The program copies configuration, setting, degrader files from the directory "Program Files\LISE " (default) in "\user\MyDocuments\LISE\". The User's ME file is created in the directory "bin". All users have then own settings of the program, as well as the nuclide file and User's ME. The database A&W95 remains common for all users, and is protected from changes.

The program compares the versions of the files in the directory "MyDocuments\LISE" to the current version of the program each time at loading. LISE++ will copy the updated files in the directory "MyDocuments\LISE" in case of a new version has been installed.

1.1.1. Using the folder "My Documents" for users with administrative privileges

If users with administrative privileges want to keep their settings in the "MyDocuments\LISE" directory they have to set the file "*lise.ini*" to "Read only". In this case ALL users will work from their "MyDocuments\LISE" directories.

1.2. "Charge", "Global", "PACE4" & "BI" for "unprivileged" users

The programs "Charge", "Global", "PACE4"also check the possibility to create files in the default directory. If the attempt is unsuccessful these programs create temporary files and read & write result files in the directory "MyDocuments\LISE\files".

2. User's Mass-Excess file

Masses of isotopes are used everywhere in the program from energy losses of ions in matter to the Brho-analyzer. It is important to use correct values of masses in evaporation cascade (*Abrasion-Ablation* and *LisFus* models), as well as in the kinematic calculator. In the previous versions masses were taken from the mass database [A&W95]. There are some disadvantages of using this database:

- If a mass excess value is changed then it is necessary to change all other cells manually;
- There is no calculated suggested value in the dialog "Database" for an isotope which is missing in the database;
- Only one database "*lise.dbf*" can be used.

In the new version of LISE++ it is possible to use other databases of masses: the user's mass excess file (UME). This file only stores mass excess value of isotopes, and other isotope characteristics that are calculated by the code. Therefore the UME file has much smaller size than the database A&W95. The UME file is called by default "*user_mass_excess.lme*" and found in the "\bin" directory. If the UME file is missing, then LISE++ will create a new UME file using information from the database A&W95.

2.1. Use of mass models

The user can choose a UME file to be used in the code in the "Production mechanism" dialog (see region "A" in Fig.1). In this dialog the user can determine a mass model to be used in future calculations. There are 9 available combinations (see region "B" in Fig.1):

1. Database+Calculations: one of two mass databases (A&W95 or UME file) + one of three available LDM to extrapolate masses of nuclei missing in the database.

2. Calculations only: one of three LDM formulas.
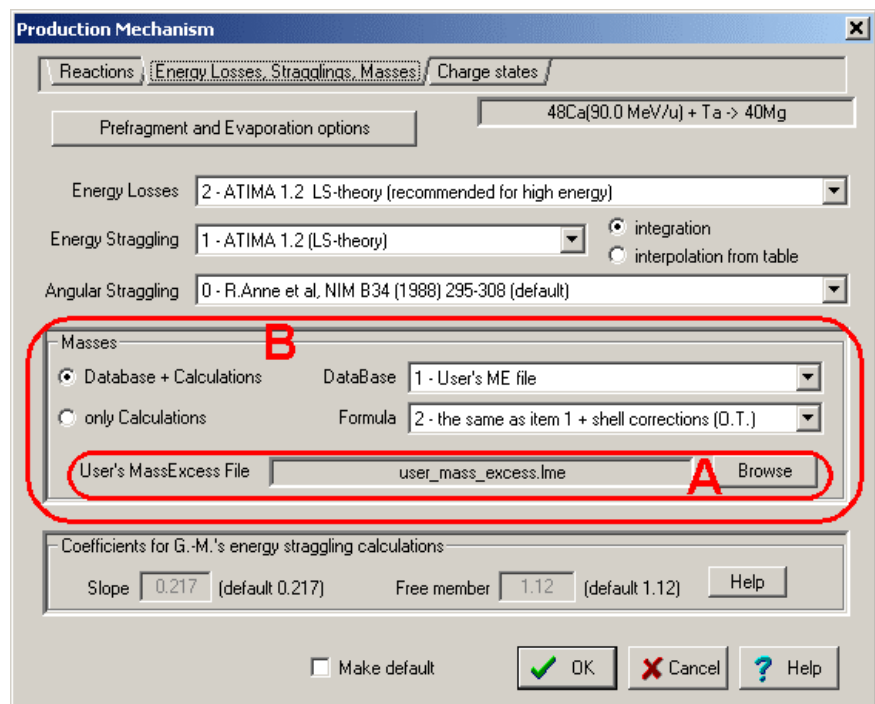
Fig.1. *The "Production mechanism" dialog: choose a mass model.*

2.2. UME file format

The format of the UME file is simple. It is an ASCII file that consists of two columns separated by one of several possible separation characters (tabulation sign, comma, or space). The first column is the isotope (Z,N) index in format $Z \times 1000 + N$. The second column is the mass excess value of this isotope in MeV. The ME value can be written in exponent form, or in floating point format.

2.3. UME file editing

New records in the UME file and changes of already existing data can be performed through the "Database" dialog from the menu "Database" (see Fig.2). The user has to choose the database mode "1-User's ME file" to obtain access to the UME file data. There are three possible states of the data (see rectangle "C" in Fig.2):

1. Data from User's ME file.

2. ME value has been modified.

3. LDM calculation.

The two first states show an already existing record. In the third state the data the isotope is missing in the UME file, and calculated values are shown in the dialog. Click "Add record" to add the calculated value for this isotope to the UME file. After the record is created it is possible to edit the mass excess value for this isotope.
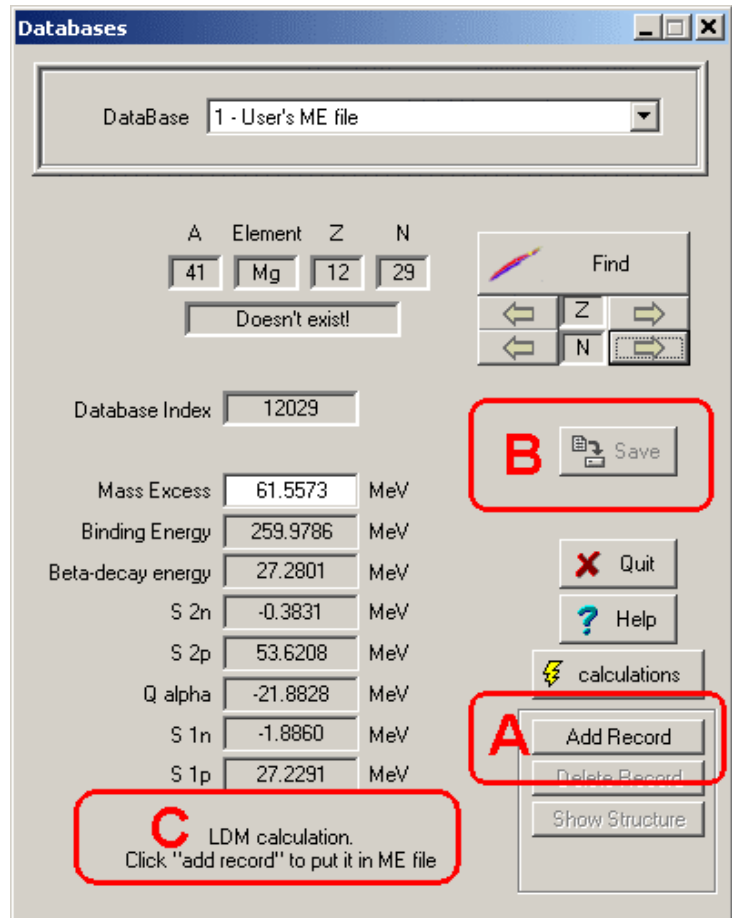
The new database of Audi & Wapstra (edition 2003) will soon be incorporated. Mass

Fig.2. The "Databases" dialog in the UME file mode.

excess errors will also be used in the code (at least for plots). Mass excess errors will be recorded in the UME file as the third column.

☞ When you are editing a mass excess value don't forget that isotope characteristics such as separation energies of neutrons or protons are also changed in the neighboring nuclei. For example, the work [Sar00]: the <u>measured</u> masses of particle-bound isotopes ^{34,35}Mg equal 9220(330) and 17540(1000) respectively. If one puts these values in the "Database" then ^{35}Mg isotope becomes unbound by 249 KeV against one neutron emission because of the large error bar on the measurements.

☞ Important details about the UME file are given in the sections in relation with the user's privileges (*1. LISE for "unprivileged" users*) and the separation energy determination through production cross-section (*4.8.* Cross-section & minimum separation energy dependence).

3. User's cross-section file

Even if the user had the cross-sections file obtained from experimental data or calculation by other programs it is possible to input cross-sections manually in the LISE++ program to be used in calculations. The new version allows users to read/write cross-section values from/to the Cross-section File (CSF).

All CSF operations are available if the option "Fit/File" in the box "Cross-section" in the "Preference" dialog is set to "File" (see Fig.3). Using the button "CS File settings" from the "Preference" dialog (Fig.3) or the menu "Options->Cross-section file" the user can load the "CSF dialog" (see Fig.4) to provide operations with the CSF.
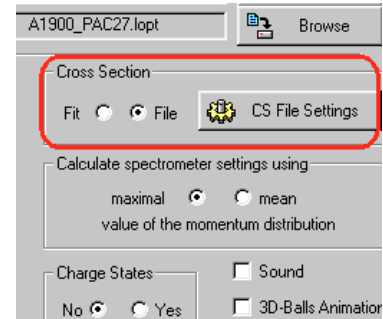
Fig.3. The "Cross-section" block in the "Preference" dialog.

The "Browse" button allows users to connect to the CSF. To **load** CS values from the connected file in the memory it is necessary to click the "Load" button. There are two options to load data:

- *Append:* already existing data in memory are saved; missing data are added in memory.
- *Overwrite:* if CS data already exist for given isotope then it will be overwritten.

☞ Use the "Remove All CS from memory" button if it is necessary to remove all data from the memory before loading data from the CSF.

If the number of user CS (or in other words "CS in memory") is not equal to zero then the "Save as" button is available. It is possible to save the data in a file with other name than the connected CSF. The connected CSF is left as the same in any case. The number of used CS is shown the dialog.

The format of CSF is simple and shown in the dialog. PACE4's CSF can be used by the LISE++, but the file has the special header which is read by LISE++ to show PACE4 settings applied to provide these calculations.

There is brief description of some buttons:
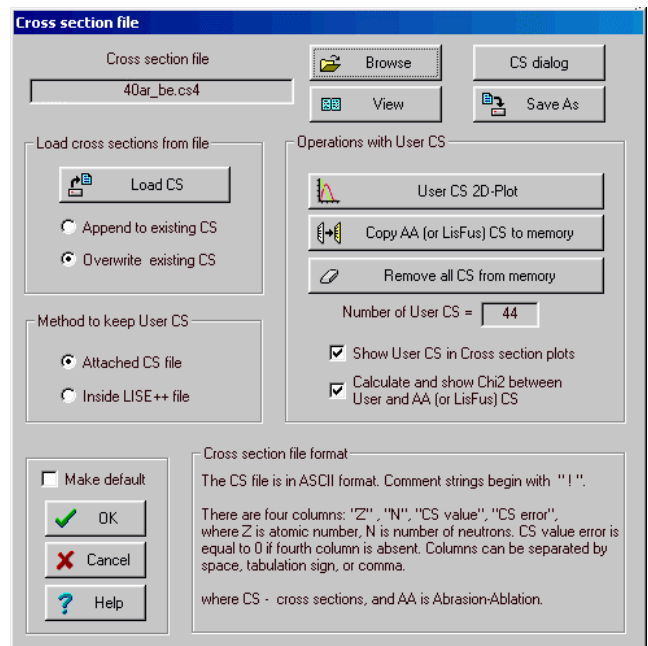
Fig.4. The "Cross-section file" dialog.

- *View:* to visualize contents of the connected file;
- *CS dialog*: to get the "Cross-sections" dialog to see cross-sections calculated by LISE++ and to modify user CS;
- *User CS 2D-plot:* to plot cross-section values loaded to memory. This command is available if at least one CS value is loaded to the memory;
- *Copy AA or (LisFus) CS to memory:* if Abrasion-Ablation or LisFus models were used to calculate CS then the user can copy them to memory (by OVERWRITE method!!). This button is not available if the number of AA (or LisFus) cross-sections is equal to zero.

☝ For fast work it is preferably to load AA (or LisFus) calculated values from "fast" CS memory then recalculate them again.

3.1. Methods to keep user CS

There are two methods to save CS values in files to use them the future:

- Inside LISE++ file: CS values are saved inside LISE++ file as it has been done in the previous versions. In this case the data increase LISE++ file size and can not be used by other applications (by default).

- Attached file: Data are kept in the connected CSF. The CSF is saved when the user clicks the button "Save As" in the "CSF" dialog *OR* the LISE++ file is saved in the disk. When the LISE++ file with the attached CSF is loading, the CS data are automatically loading from the CSF to the memory. It is possible to see the name of the connected file in the "Setup" window (see Fig.5) if the number of memory (User's) cross-sections is positive, the option "Cross-sections" is set to the value "File" (see Fig.3), and the method to keep user CS is set to "Attached CS file".
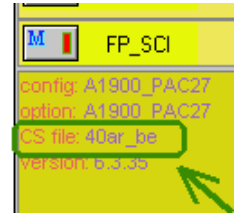
Fig.5. The fragment of the "Setup" window shown the connected CS file.

3.2. User CS in plots

User CS data are plotted (Fig.6) if the option "Show User CS in Cross-sections plot" is set in the "CSF" dialog (see Fig.4). Errors of user CS data are plotted also if they are different from zero (see fragment "A" in Fig.6). Chi-square calculation results between User CS and AA (LisFus) calculations appear in the right bottom corner of the plot if the option "Chi-square" is set in the "CSF" dialog, and at least one isotope from memory CS exist for which AA calculations was done. The value "*LoD*" shows an average deviation in log-scale $LoD = \sum_{i=1}^{N}\left|\log 10(y_{exp}) - \log 10(y_{calc})\right|/N$
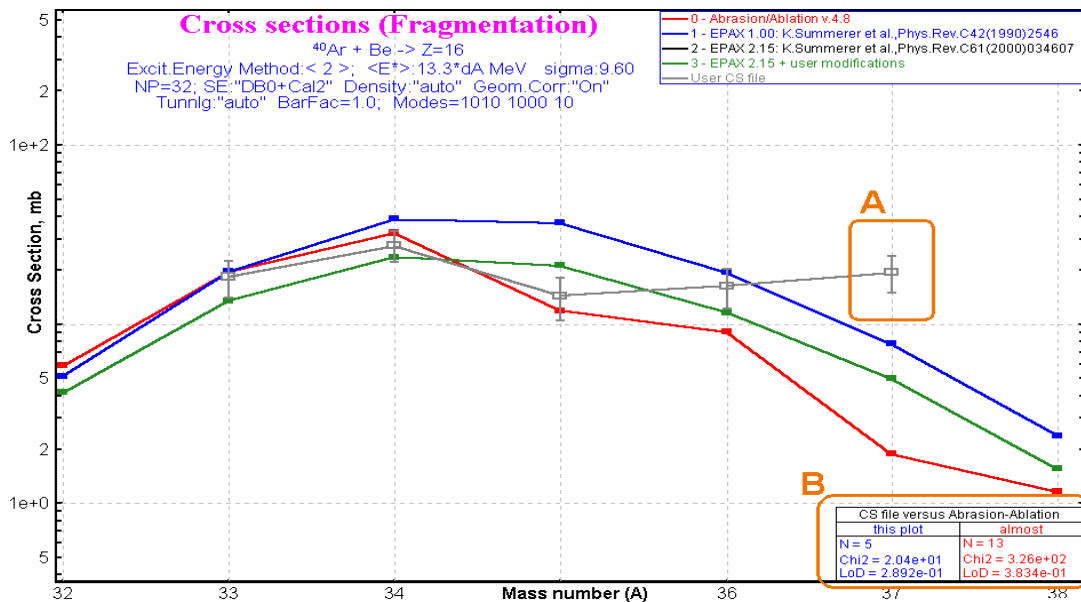
Fig.6. The cross-section production plot for Z=16 in the reaction $^{40}Ar+Be$.

4. Abrasion-Ablation revision

The AA model has undergone significant updates in the new version, both for the first part of model (excitation energy), as well as for the evaporation cascade. The new options, new plots have been implemented, and some corrections were done. The algorithm of determination of excitation energy parameters compared with experimental data is presented. All this is presented in this chapter step by step using examples. At the end of the chapter the comparisons of experimental data and calculations for several primary beams are shown. Three step fragmentation process and separation energy determination through production cross-section of fragment are discussed.

4.1. Evaporation cascade

To understand the AA new features it is better to begin with the "Evaporation calculator" in the mode "Excited nucleus evaporation" (see Fig.7, step 1). Let's consider an [40]Ar nucleus (step 2 in Fig.7) with excitation 40-45 MeV (rectangle distribution). To observe the complete evolution of the cascade, set the final nucleus also to [40]Ar (step 3). To begin calculations use the button "Calculation" (step 4). To get the plots as shown in Fig.8 and Fig.9 use the button "Excitation energy plot" (step 5).
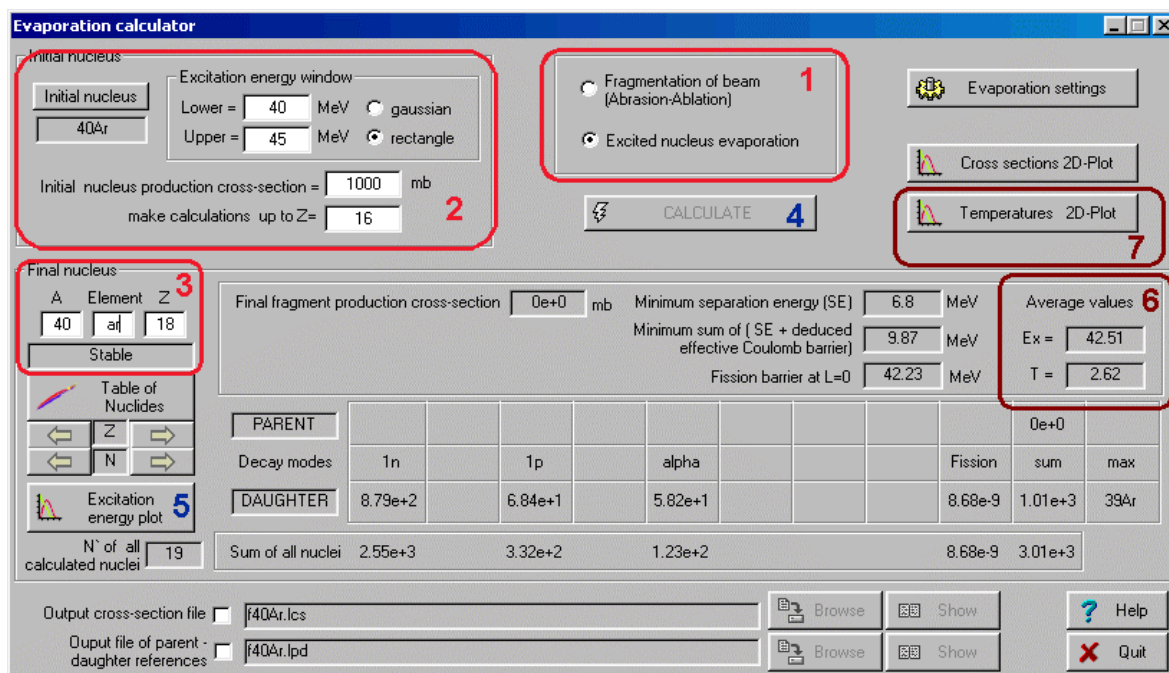
Fig.7. The "Evaporation calculator" dialog in the mode of "Excited nucleus evaporation".

1. The left top plots in Fig.8 and Fig.9 represent the sum of initial and parent excitation energy distributions. In the case of Fig.8 there are not parent distributions, because the sum distribution is equal to initial one defined as a rectangle from 40-45 MeV in the Evaporation calculator.

2. The left bottom plots in Fig.8 and Fig.9 are new in the new version and show the evaporation channels in the excited nucleus. The area painted in dark blue shows the cross-section of the residue production. All the cross-section to the right of this area goes to the daughter nuclei. The "sum" distributions in the left figures are identical. However, the top figure shows how it was produced, and the bottom figure how it breaks up.

^{40}Ar excitation distributions

Excit.Energy: 40.0-45.0 MeV; Fus.CS: 910.1 mb; Fus.Barrier: 10.95 fm; h_omega = 5.0 MeV

NP=32   SE:"DB0+Cal2" St.Density:"auto" Geom.Corr:"On" Tunnlg:"auto"   Modes=1010 1000 10

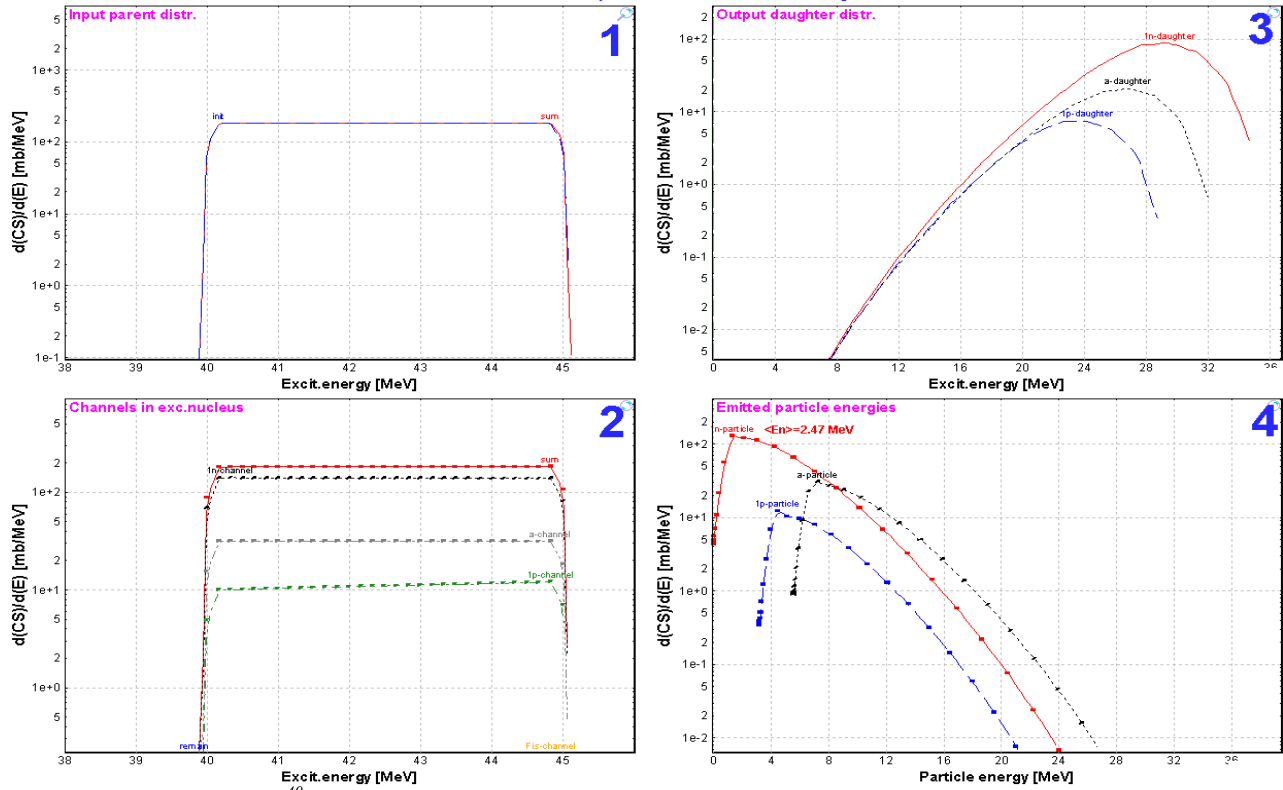**Fig.8.** ^{40}Ar excitation distribution plots created from the Evaporation calculator.

^{38}Cl excitation distributions

Excit.Energy: 40.0-45.0 MeV; Fus.CS: 910.1 mb; EVAPORATION - Initial nucleus ^{40}Ar

NP=32   SE:"DB0+Cal2" St.Density:"auto" Geom.Corr:"On" Tunnlg:"auto"   Modes=1010 1000 10

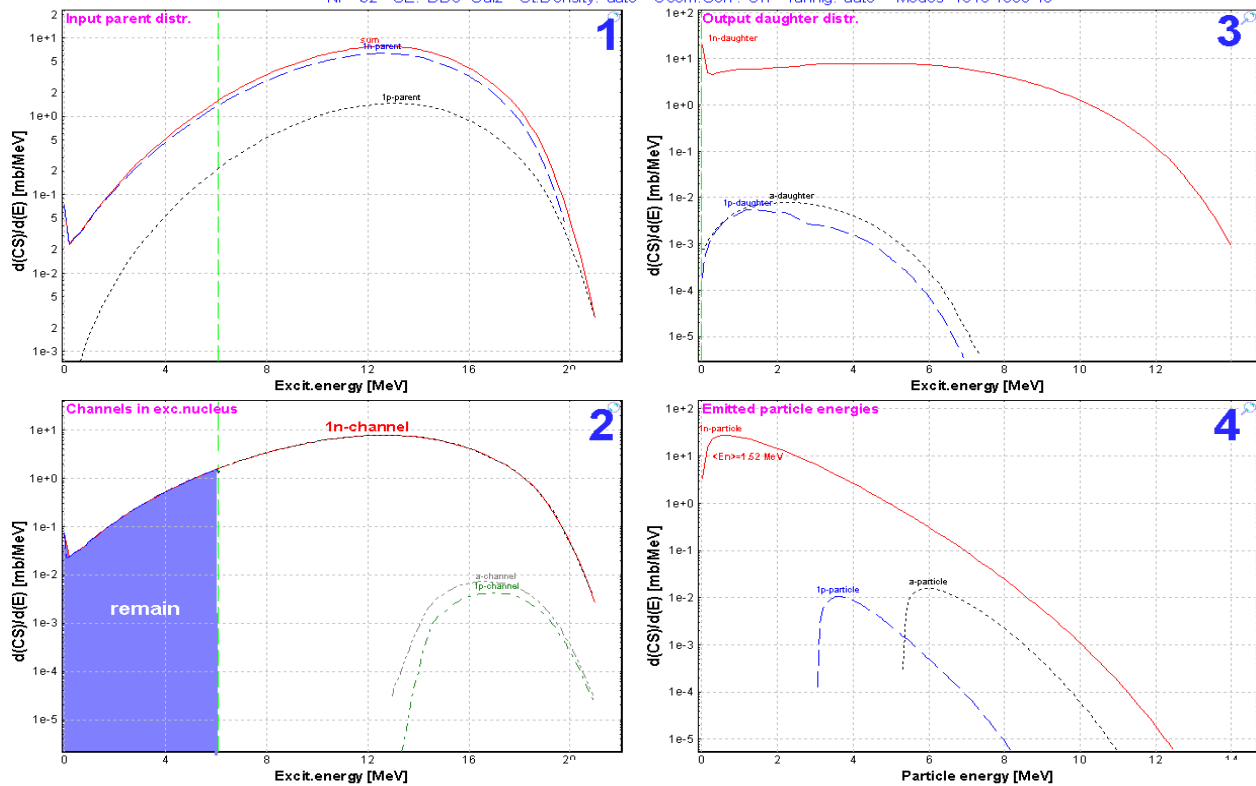**Fig.9.** ^{38}Cl excitation distribution plots created from the Evaporation calculator.

The green vertical lines on the left plots show the minimum separation energy and the minimal sum of separation energy and effective coulomb barrier. If the minimal separation energy is less than zero (in case of proton-rich nuclei or heavy nuclei), then the fission barrier is shown instead of the minimal separation energy.

3. The right top plots in Fig.8 and Fig.9 show the excitation energy distributions in daughter nuclei.

4. The right bottom plots are also new in the program and show the energy distribution of emitted particles. Using these plots it is possible to estimate the average energy of evaporated neutrons to be compared with experimental result of temperature measurements. The mean values of the average neutron energy are shown in the right bottom plots of Fig.8 and Fig.9.

The areas under the same name distributions in plots 2,3,4 (Fig.8 and Fig.9) are normalized on the one value which determines the cross-section of the evaporation channel.

To estimate the channel widths the code uses the average values of evaporated particles. However to create the daughter excitation energy distributions the code can

A) use the time-consuming qualitative approach using energy distribution of evaporated particles as it has been done for plots Fig.8 and Fig.9, or
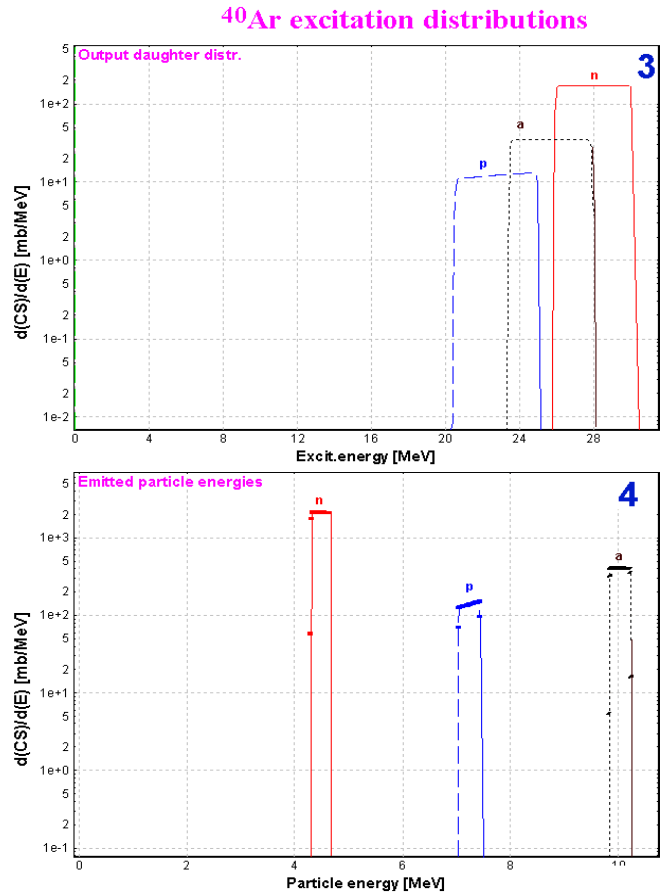
Fig.10. The ^{40}Ar excitation distributions plots are the same as right plots in Fig.8, but the daughter excitation energy distributions were calculated using the average value of emitted particles.

B) apply an average energy value of emitted particles as shown in Fig.10. This new option can be applied for the highly excited heavy nuclei to make calculations faster.

It is possible to choose the calculation mode of the daughter excitation energy distribution in the "Evaporation (Prefragment) options dialog" (see Fig.11, "A").

Fig.11. The Evaporation (Prefragment) options dialog

4.2. Corrections of low energy region

4.2.1. Level density

The nuclear level density (non-collective nuclear internal excitations) is described by the Fermi-gas expression [Ilj92]:

$$\rho(U) = \tfrac{1}{12} \sqrt{\pi}\, a^{-1/4} (U - \Delta)^{-5/4} \exp\!\left(2\sqrt{a(U - \Delta)}\right) \hspace{2cm} /1/$$
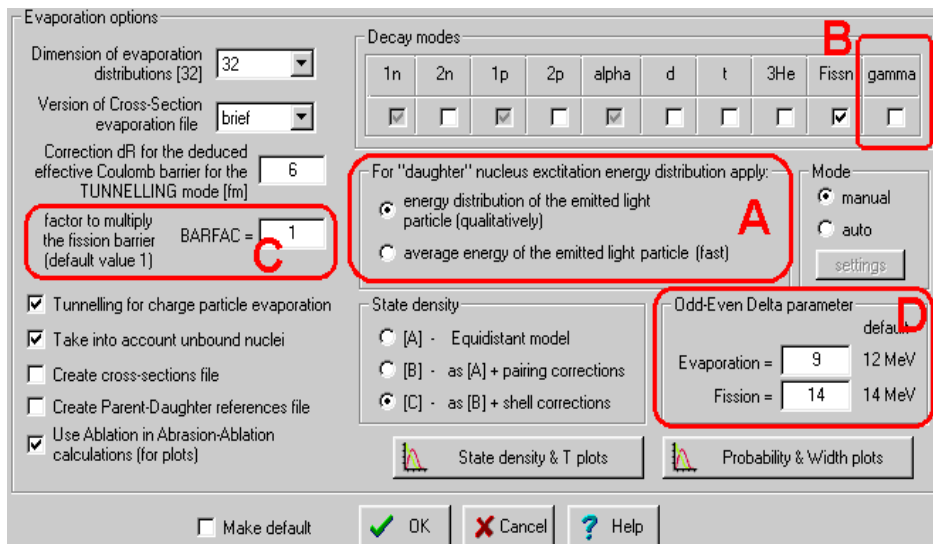
where a is the level density parameter, and Δ is the pairing energy. Let's consider the behavior of that expression at small energies (see the blue curve in Fig.12):

- It is invalid for energy $U < \Delta$;

- It has a minimum at $U_{min} = \tfrac{25}{16} a + \Delta$ (assuming that a is independent from U);

- It diverges to infinity when U comes nearer to a point Δ $(U > \Delta)$.

The pairing energy Δ explains the fact that for even-even nuclei the first exited level is relatively high. At lower level density the value Δ is assumed to be equal to 0. The levels density is used to calculate the evaporation channel, but in the case of an excitation energy lower than Δ it follows from equation /1/ that this channel is closed. Let's consider the case of a particle-unbound nucleus with populated low-energy state (for example ^{25}O in Fig.13). The neutron evaporation channel from ^{25}O is closed as the level den-

Fig.12. *Plot of level density versus excitation energy. The blue curve shows the calculation by formula /1/ with pairing corrections. LISE's extrapolation is shown by the red curve.*

sity of ^{24}O nucleus is equal to zero for such small excitation energy, and therefore the unbound nucleus becomes artificially particle-bound. It means that the possibility to go in the ground state of the daughter nucleus is missing. To avoid this problem, a linear extrapolation of level densities has been implemented in the code LISE++ from zero up to the energy $U_B = \tfrac{3\cdot25}{16} a + \Delta$ using the values at points U_B and $U_B + 2$ MeV (red curve in Fig.12).

Fig.13. *Example of slightly excited particle-unbound nucleus. The left picture shows the restriction of n-evaporation channel in the case $\rho=0$ based on expression /1/. On the right picture the level density is not equal to 0 according to LISE's extrapolation, consequently the n-evaporation channel is allowed.*

4.2.2. Temperature

The same problems as with the level density at low energies appear in the case of the temperature calculation with the implementation of the pairing correction Δ:

$$T(U) = \sqrt{(U - \Delta)/a} \qquad /2/.$$

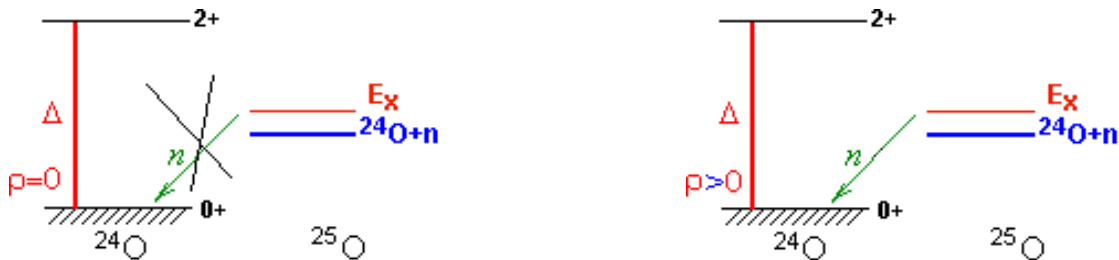The temperature for an excitation energy lower than Δ should be small, but not equal to 0. Experimental data cited in the work [Ilj92] have chosen the criterion $U - \Delta \geq 2MeV$. Keeping the same distance s (2 MeV) from the value Δ it was decided to enter in the code LISE++ a function $f(U)$ which satisfies the following:

1. the function $f(U)$ is continuous in the region $0 \div (\Delta + s)$;

2. $f(0)=0$, and $f(U)>0$ for $U>0$ and $U<(\Delta+s)$

3. $f(\Delta+s)=T(\Delta+s)$, and $f'(\Delta+s)=T'(\Delta+s)$;

A polynomial of second order was chosen as the simplest choice. The polynomial coefficients are determined using the second and third criteria. The resulting temperature dependence from excitation energy is shown in Fig.14.
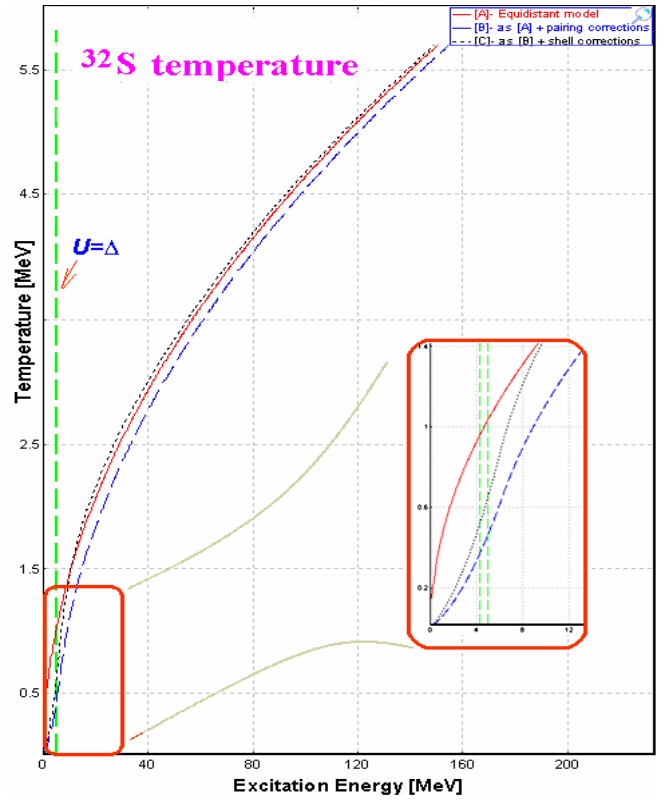

Fig.14. ^{32}S temperature dependence from excitation energy.

4.3. γ-channel in evaporation cascade

At first approximation the nucleus angular momentum was neglected and it was assumed that dipole $E1$-transitions are the main source of γ-quanta from highly-excited nuclei. In the statistical model for the partial width Γ_γ the following expression is used:

$$\Gamma_\gamma(U_L) = \frac{3}{(\pi\hbar c)^2} \frac{1}{\rho_0(U_0)} \int_{U_L}^{U_0} \sigma_\gamma(E)\rho_\gamma(U_0 - E)E^2 dE \qquad /3/$$

where E is the energy of γ-quantum, U_0 is the excitation energy of nucleus, $\sigma_\gamma(E)$ is the dipole photoabsorption cross-section. The total partial γ-width is used to calculate for U_L=0. A probability to emit **one** γ-quantum with the remaining excitation energy in the nucleus minus the minimum separation energy S_{min} in the nucleus can be calculated taking U_L equal to $U_0 - S_{min}$. In other words the $\Gamma_\gamma(U_0 - S_{min})$ defines the survival cross-section of this excited nucleus. If the γ-channel is switched off and $U_0 < S_{min}$ the code assumes no more decay (see the left bottom plot in Fig.9). A zero value is used in $\Gamma_\gamma(0)$ for partial widths calculation in the "Widths plot" in the "Evaporation option (Prefragment)" dialog. The gamma-channel has been implemented in the evaporation cascade in the new version (see Fig.11, fragment "B"). In this mode the low limit U_L is taken equal to $U_0 - S_{min}$ for $\Gamma_\gamma(U_L)$ calculations. It is advised to use this option carefully because the γ-channel assumes an $E1$-transition, and rotational and vibrational collective enhancements, as well as angular momentum are not taken into account in the code. Therefore the gamma-channel is turned off by default.

4.4. Calculation of temperature in Evaporation calculator

The Evaporation calculator dialog has been modified to show the temperature of the excited nucleus. The average temperature shown in Fig.7 (region 6) is calculated based on the average value of the excitation energy distribution. It is possible to see a small difference between this calculated value and the temperature extracted from the average kinetic energy of neutrons (see the right bottom plots in Fig.8 and Fig.9.). Using the button "Temperatures 2D-plot" (Fig.7, region 7) the user can visualize a temperature map of all nuclei participating in the evaporation cascade (see Fig.15), as well as to compare the temperature map with the cross-section plot (see Fig.16).
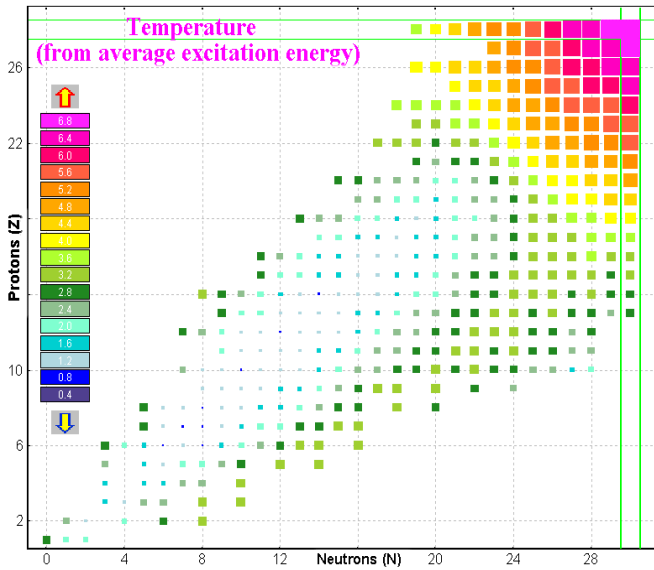

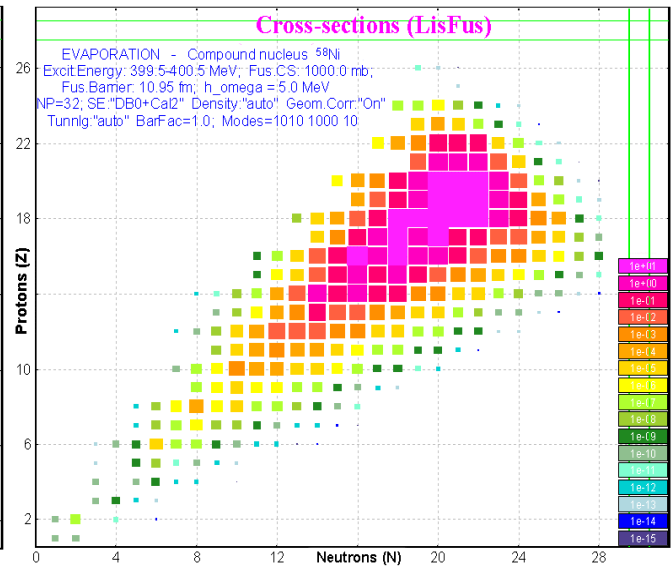**Fig.15.** *Temperature plot of ^{58}Ni nucleus deexcitation (E_x=400MeV).*

Fig.16. *Residues production cross-section plot in the case of excited nucleus ^{58}Ni (E_x=400MeV).*

4.5. "BarFac" - fission barrier coefficient

The fission barrier coefficient "*BarFac*" (By analogy with the program PACE) has been added in the Evaporation option dialog (see Fig.11, fragment "C"). The "*BarFac*" value is taken as a factor to multiply the fission barrier. The experimental [Oga98] fusion-evaporation cross-sections for reactions $^{48}Ca(^{206}Pb,1-3n)$ and $^{48}Ca(^{208}Pb,2n)$ and "LisFus" calculations are shown in Fig.17. The "BarFac" value was set to 3.9 (!!) in the LisFus calculations to be compared with the $^{48}Ca(^{206}Pb,2n)$ experimental data. This emphasizes the necessity to reconsider the fission barrier model in the program.

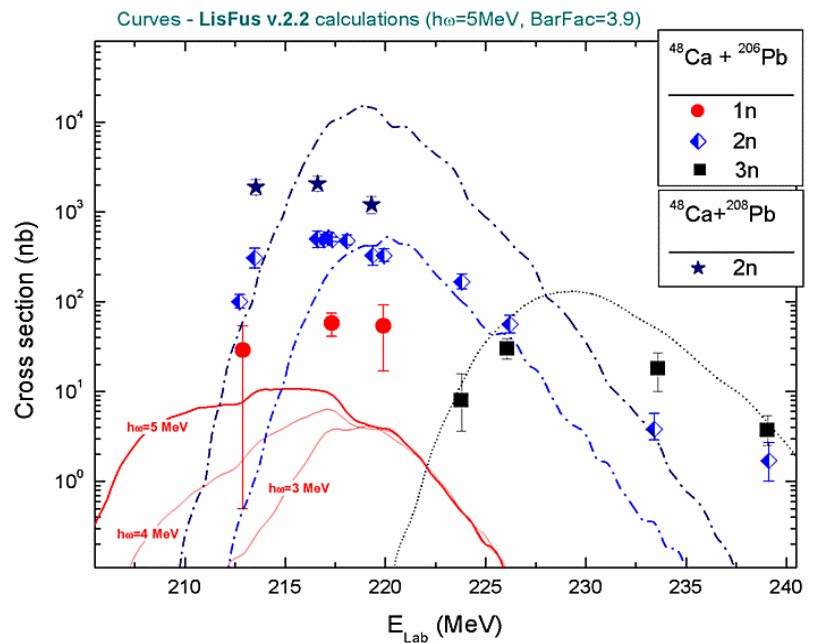**Fig.17.** *The experimental [Oga98] fusion-evaporation cross-sections for reactions $^{48}Ca(^{206}Pb,1-3n)$ and $^{48}Ca(^{208}Pb,2n)$. The curves are showing the "LisFus" calculations used with the settings: BarFac=3.9, hω=5MeV.*

4.6. Excitation energy of prefragment

The method "C" of prefragment excitation energy has been modified in the new version in order to TRY to describe the excitation energy distribution proposed by K.-H.Schmidt et al. [Sch02] and shown in Fig.18. The boundary between two regions called "L" and "H" can be built from the atomic number Z as well as the mass number A (see Fig.19).
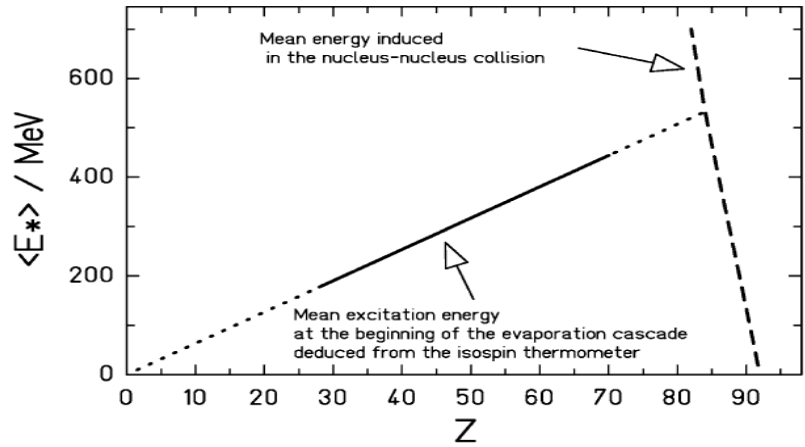

Fig.18. *Schematic presentation of the initial energy induced in the abrasion stage and of the mean excitation energy at the beginning of the evaporation cascade after fragmentation of ^{238}U in a lead target [Sch02].*

The mean value and width of excitation energy distributions can be expressed by a second order polynomial. Actually just coefficient of the first order is used then a second order coefficient and a free member are equal to zero in these polynomials.

The plot of temperature versus mass number has been implemented in the code to help choose and set the excitation energy model (see right bottom plot in Fig.20). The modified model "C" of prefragment excitation energy in "L"-region is set to a temperature equal to 3.4 MeV (see Fig.20), that corresponds to an excitation energy E_x=1.6·A.

It is possible to turn on/off the LISE corrections for the Geometrical AA model (see fragment "C" in Fig.19). The left bottom plot shows cross-section values versus the prefragment mass with the LISE corrections (red and black curves) and without them (blue curve).
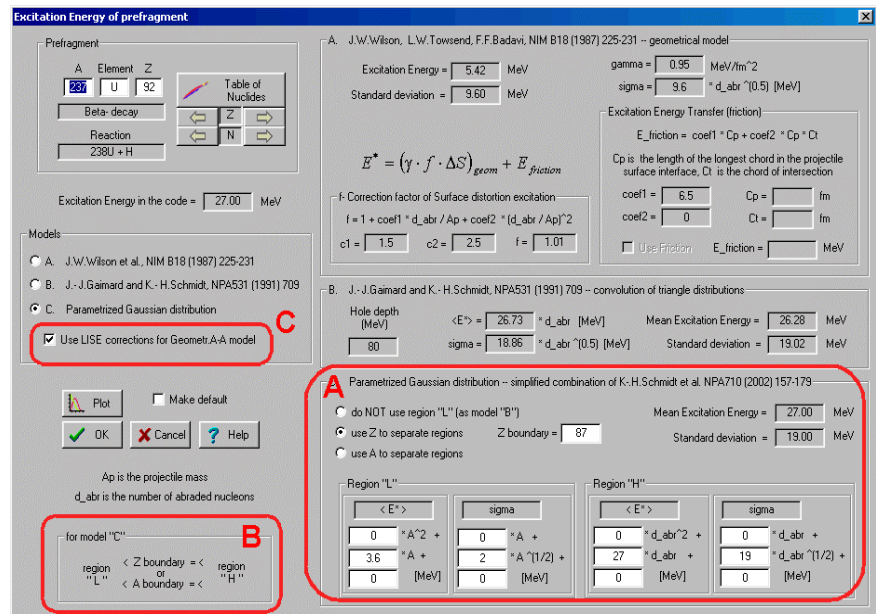

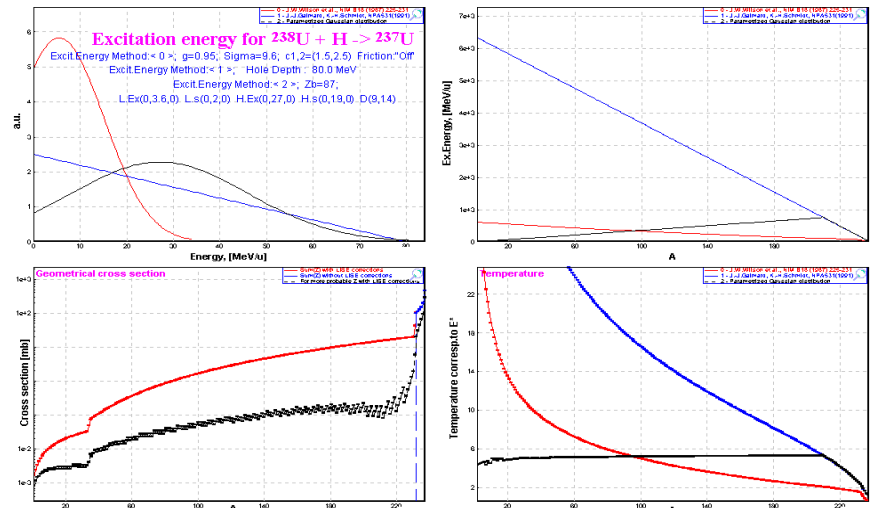**Fig.19.** *The "Excitation energy of prefragment" dialog.*

Fig.20. *Excitation energy and temperature plots created from the "Prefragment excitation energy" dialog.*

4.7. Comparison with experimental data

In order to compare experimental results in LISE++ with calculations it is necessary:

- Save experimental production cross-section values in the CSF (3. User's cross-section file).
- Load cross-section values from the User CSF to memory to be used in LISE++.
- Create cross-section plots to see comparison results (*Chi*2 or *LoD*) between calculated and experimental cross-sections (see fragment "B" in Fig.6)

It is planned to create a possibility to use a batch-file in LISE++ with different initial settings to fit experimental data. The user can adjust the parameters only manually in this version.

4.7.1. $^{58}Ni+Be$

Experimental results from works done in GSI [Bla94] and NSCL [Moc03] (preliminary) were used for analysis. A primary beam of ^{58}Ni at 650 MeV/nucleon was used to measure production cross-section of proton-rich fragments in GSI, whereas the beam energy in NSCL experiment to study neutron-rich fragments was 140 MeV/nucleon. 152 production cross-section values in the region of atomic number Z=10-28 were analyzed. The minimization of the reduced parameter RP=[Chi2+ (LoD-0.1)·2000] (for *LoD* definition see 3.2. User CS in plots) is used to obtain the AA parameters for this set of experimental data.

The next options and parameters of AA model were kept in analysis:

Dimension of evaporation:	32	Geom. corrections:	yes
Decay Modes:	1n,2n,1p,2p,α	BarFac:	1
State density:	C	Masses:	Database1 + LDM2
Take into account unbound nuclei:	Yes	Excitation energy method:	C

4.7.1.1. Step 1: Excitation energy

An average excitation energy of 27 MeV per abraded nucleon was used in the work [Bla94] to reproduce the experimental data. Six different values of excitation energy 27, 20, 16.5, 13, 9.5, 7 were used in our analysis. The values σ were searched from the minimum of *RP* value for each of excitation energy value. The minimum of *RP* value is reached for $<E>$=9.5, and σ=5 with the excitation energy option "Don't use region "L"".

Excitation energy model "C"		Tunneling	Odd-even shift	Results		
$<E>$	σ	dR	Δ_0	*Chi2*	*LoD*	***RP***
27	**19.1**	Auto	12	1010	0.4997	**1809**
9.5	**5**	Auto	12	794	0.4367	**1467**

Where dR and Δ_0 are described in the next chapters.

Conclusion 1: An average excitation energy is considerably less than it was found in the work [Bla94].

4.7.1.2. Step 2: Deduced effective Coulomb barrier

The *dR* correction for the deduced effective Coulomb barrier for tunneling model was determined to be equal to 6 *fm* in work [Ben98]. Increasing the effective barrier (by decreasing *dR*) leads to increasing reduced minimum separation energy for proton-rich isotopes and as a consequence the increase of production cross-section of this fragment. In the first versions of AA-model in LISE it was assumed that *dR* correction is equal to 0 for light prefragments. The parameterization for *dR*-value was proposed for "AUTO-mode" (http://groups.nscl.msu.edu/lise/5_8/lise_5_8.html#g1).

The large discrepancy (see Fig.21) was noted for proton rich fragments from visual comparison of AA calculations (after the first step) and experimental data what can be corrected by the effective reduced Coulomb barrier. The option "AUTOmode" was used in the first step to calculate *dR* value. This correction calculated by "AUTOmode" is equal to 2.7 in mass region 50. In the second step AUTOmode was switched off, and the correction *dR* was set manually.
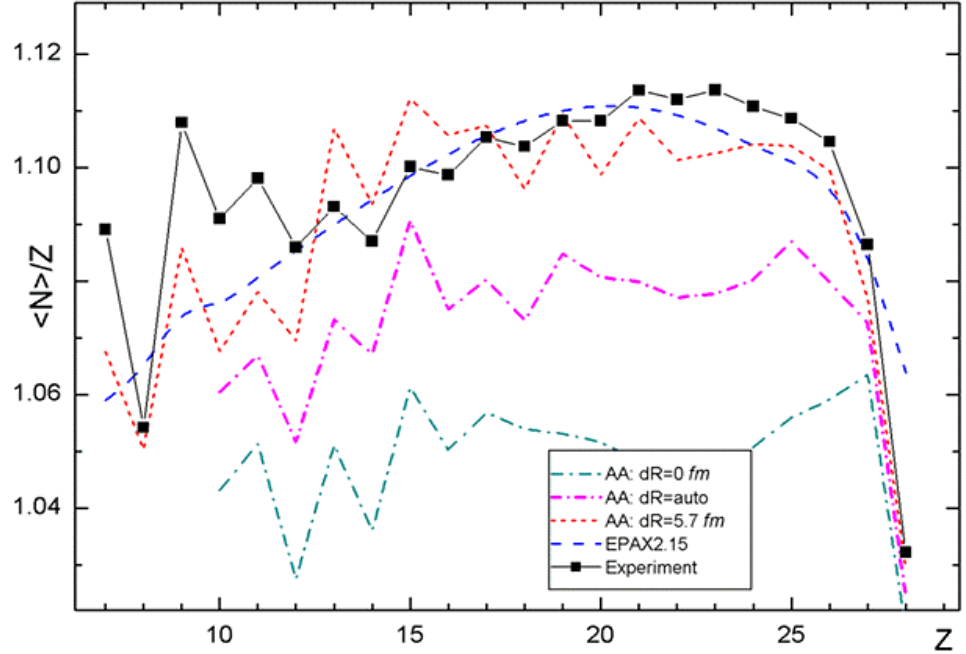

Fig.21. *Experimental data neutron-over-proton ratios of heavy fragmentation-evaporation residues produced in the fragmentation of ^{58}Ni+Be in comparison with the results of EPAX 2.15 and LISE++ Abrasion-Ablation 5.0 using different values of the correction radius dR.*

Excitation energy model "C"		Tunneling	Odd-even shift	Results		
<E>	σ	*dR*	Δ_0	*Chi2*	*LoD*	*RP*
8.5	**4.6**	**5.75**	12	340	0.2887	**717**

The final fit value *dR* is close to results of analysis [Ben98]. It is recommended in the future LISE++ AA calculations to use the fixed value of *dR* correction instead "AUTOmode" option. Difference in definition of value *dR* between versions v.5.8 and v.6.4 can be explained by the total revision Abrasion-Ablation model done in the latest versions.

Conclusion 2. The correction of effective Coulomb barrier is not dependent on mass fragment and its value is found to be equal to about 6 fm, as what determined early in work [Ben98].

4.7.1.3. Step 3: Effect of pairing correlations

The resulting washing-out of pairing correlations was parameterized by Ignatyuk et al. [Ign85]. For the differences between odd-odd, odd-mass and even-even nuclei it was proposed a backshift using the pairing gap $D_0 \approx \Delta_0 / \sqrt{A}$, where $\Delta_0 = 12 MeV$. It is possible to edit this parameter as well as the shift in the case of fission channel in the new version of LISE++ (see Fig.11, region "D").
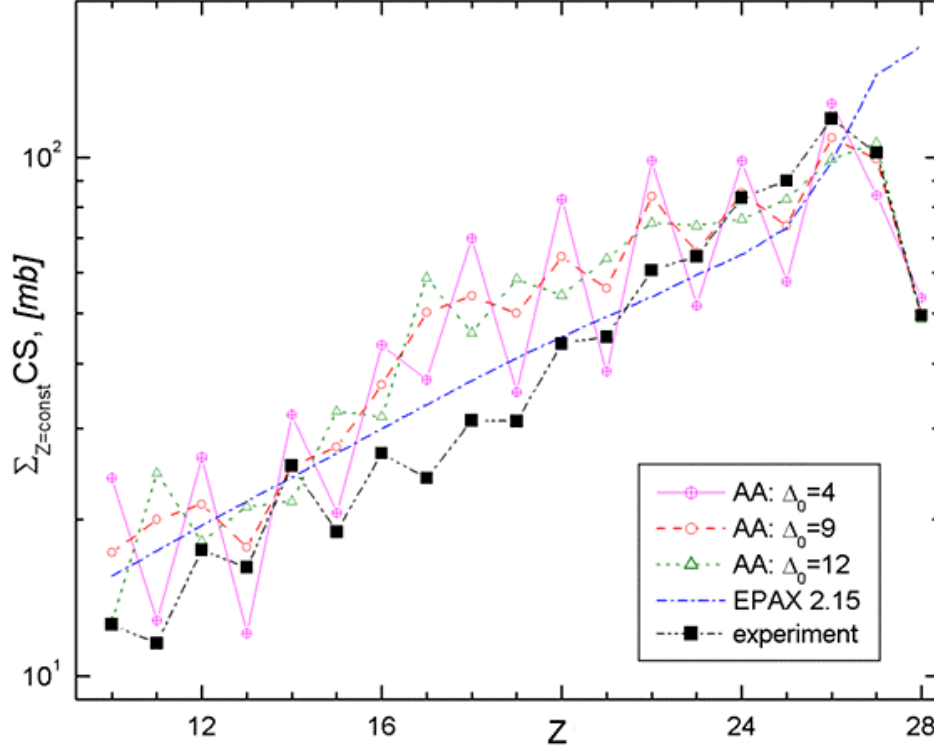

Fig.22. *Plot of the value* $f(Z) = \sum_i \sigma(A_i, Z)$ *versus the atomic number in the reaction* $^{58}Ni+Bi$.

Abarasion-Ablation calculations were done using different odd-even shift parameter Δ_0.

It was noticed from plots that some even elements have output less than their odd neighbors (for example see Fig.22). It is possible to explain by "over"washing-out of pairing correlations. The minimum of *RP* value in the case of odd-even shift Δ_0 modification has been reached for parameters shown in the following table:

Excitation energy model "C"		Tunneling	Odd-even shift	Results		
<E>	σ	*DR*	Δ_0	*Chi2*	*LoD*	***RP***
9.0	**5.0**	5.8	**9**	212	0.2062	**424**

Conclusion 3. The odd-even shift parameter Δ_0 should be lower in the fragmentation of ^{58}Ni on Be-target (see Fig.22) than it was proposed by Ignatyuk [Ign85].

4.7.1.4. Step 4: Use of two excitation energy regions

The definition of two excitation energy regions in the first time was given by K.-H.Schmidt et al. [Sch02] for an explanation of the three stage model then the temperature of 5 MeV is reached in the abrasion, and the break-up sets in. In the case of the fragmentation of ^{58}Ni on Be target after the third step of minimization presented in this work the large discrepancies between experimental results and Abrasion-Ablation calculations are observed in the region Z=8÷12. It is necessary to note that the LISE geometrical corrections were applied in the previous steps to avoid a jump (see Fig.23) caused of that a geometrical cross-section of a prefragment with mass 37 and lower in the case of the "light" beryllium target is equal to zero. The same model of two excitation energy regions as shown in Fig.18 was used in the step 4 to improve cross-section calculations of light mass fragments.
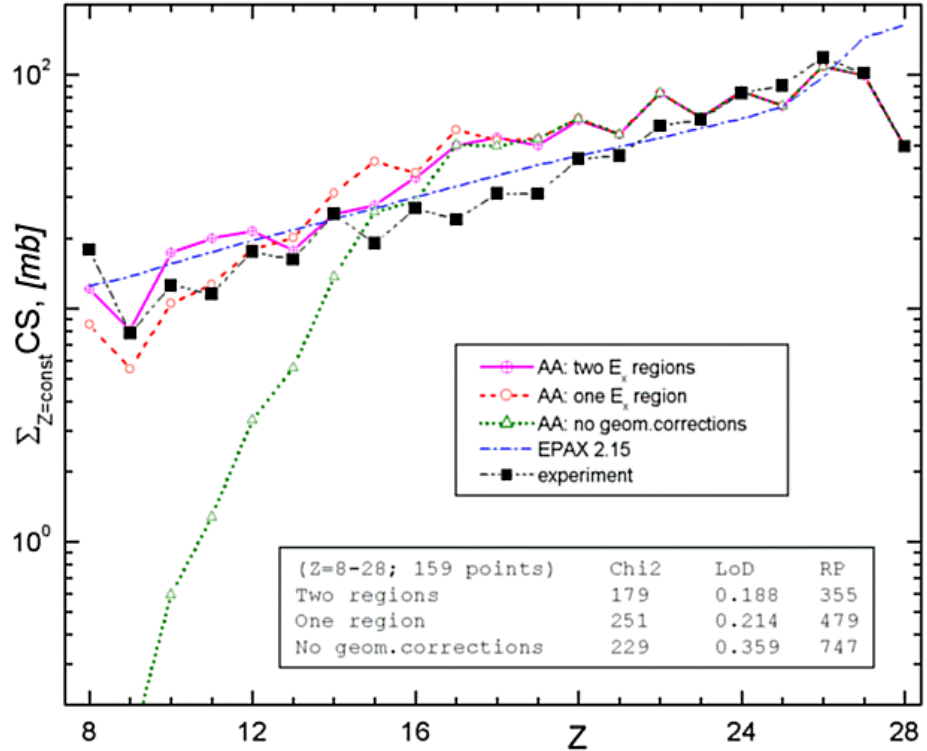

Fig.23. *The same as Fig.22 but Abrasion-Ablation calculations were done using one-region and two region excitation models. For one-region model calculations were done with and without LISE geometrical corrections for light targets.*

The border between two regions was found for prefragment mass equal to 41. The minimization results are the following:

Excitation energy model "C"				Tunneling	shift	Results		
"H" region		"L" region		Ab	dR	Δ_0	Chi2 N=152	LoD	RP
$<E>$	σ	$<E>$	σ						
9.1	5.	3.7	3.1	41	5.7	9	176	0.1890	**354**

Conclusion 4. The implementation of the second excitation energy region considerably reduces *RP*-value and improves a quality of cross-section calculations in the region of light mass fragments.

In this connection it is interesting to see the influence of the two excitation energy regions model in the case of "heavy" target where geometrical corrections are not needed.
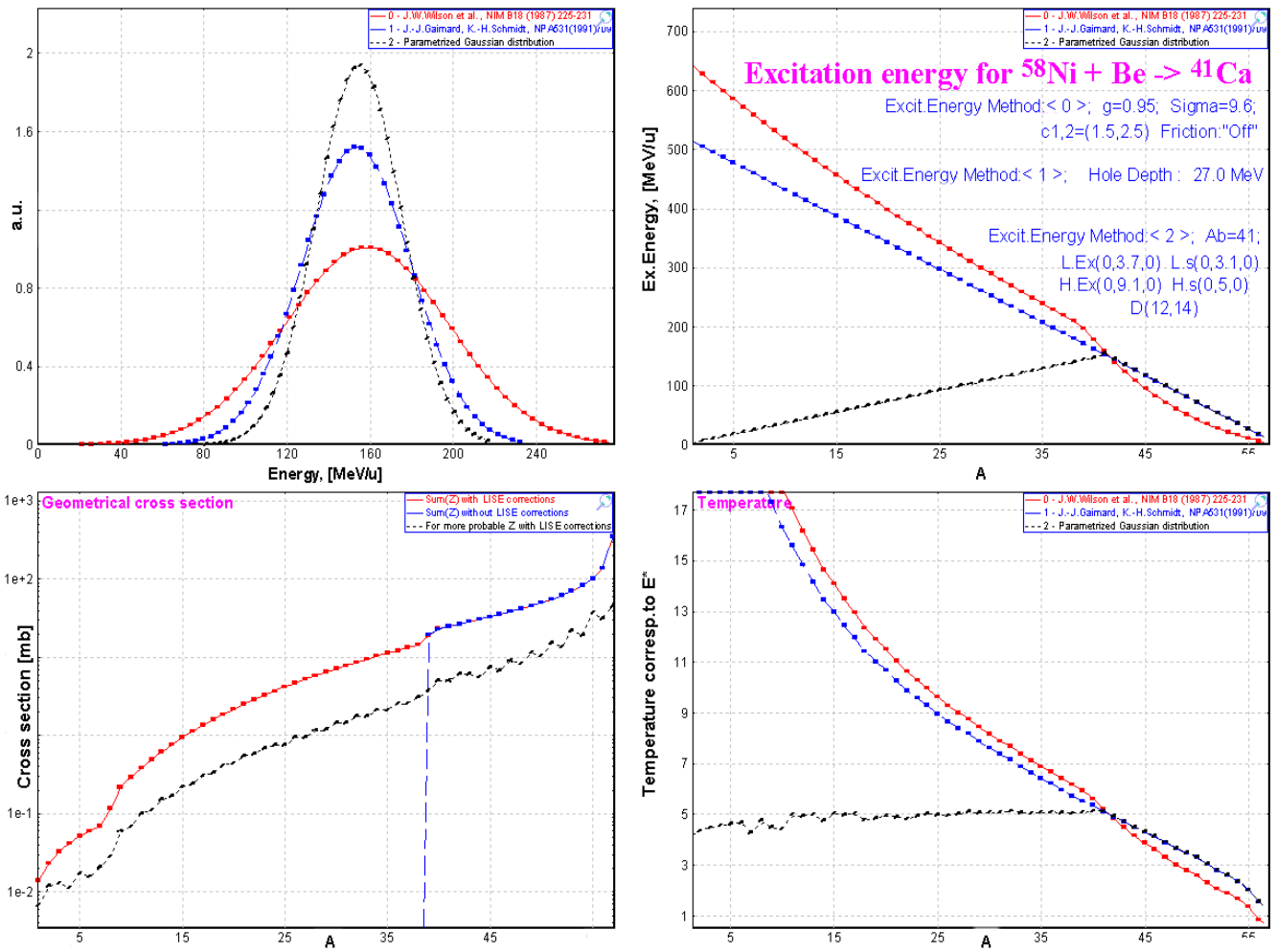
Fig.24. *Excitation energy and temperature plots created from the "Prefragment excitation energy" dialog after the fourth step of minimization with the final settings of excitation energy*

Fig.24 demonstrates final excitation energy and temperature distributions obtained as a result of minimization. Two surprising and interesting observations can be taken out from this figure:

1. The temperature in the left excitation energy region is about **5 MeV** (see the right bottom plot in Fig.24) what in K.-H.Schmidt three stage model corresponds to the temperature for the break-up set in.

2. Average values and standard deviations of excitation energy of both regions in the boundary point are approximately equal (see Table 1) though they were modified independently in minimization process!

Table 1. Excitation energy values at the boundary point A=41.

Excitation energy	"L" - region		"H" - region	
Mean value	$<E>=3.7$	$<E_{tot}>=<E>·A_{pf}=$**152**	$<E>=9.1$	$<E_{tot}>=<E>·A_{abr}=$**155**
Standard deviation	$\sigma = 3.1$	$\sigma_{tot} = \sigma·\sqrt{A}=$**19.9**	$\sigma = 5.0$	$\sigma tot = \sigma·\sqrt{A_{abr}}=$**20.6**

4.7.1.5. Results

Minimization results for isotopes and for isotones are given in Table 2. It is possible to see that the principal discrepancy in minimization is observed for isotopes in the rectangle with Z=17-19 and N=17-20. The sum of *chi2* result for these 12 nuclei makes half of total sum of *chi2* for 159 nuclei. Nowadays we are not ready to explain this appearance.

Table 2. *Final minimization results*

Z	Points	Chi2	LoD	RP1
28	8	4.47	0.163	24
27	8	11.9	0.165	38
26	11	2.24	0.117	7
25	10	4.86	0.107	9
24	12	2.72	0.129	10
23	11	7.08	0.144	20
22	14	15.5	0.206	42
21	12	7.77	0.260	47
20	11	27.4	0.375	**103**
19	6	17.2	0.265	**83**
18	7	16.2	0.240	**69**
17	8	27.1	0.336	**108**
16	6	7.52	0.124	25
15	5	7.76	0.246	58
14	4	0.832	0.092	1
13	4	1.33	0.098	5
12	5	1.81	0.079	1
11	4	9.15	0.181	55
10	4	3.42	0.148	25

N	Points	Chi2	LoD	RP1
30	7	6.31	0.203	32
29	9	3.16	0.200	23
28	9	12.3	0.297	56
27	9	2.7	0.207	24
26	9	2.81	0.138	12
25	9	4.13	0.133	13
24	11	11.1	0.179	29
23	12	12.2	0.220	37
22	11	13	0.172	30
21	11	7.12	0.149	18
20	10	38	0.292	**90**
19	10	23.1	0.213	**54**
18	6	16.6	0.279	**72**
17	5	6.33	0.188	34
16	5	0.342	0.100	1
15	4	2.37	0.126	13
14	4	0.21	0.036	-11

A comparison of experimental data and calculated by EPAX2.15 and LISE ++ AA is given in Fig.25. LISE++ file with final settings and experimental cross-sections (attached file) is located in NSCL web-server: http://groups.nscl.msu.edu/lise/6_4/examples/58ni_be.lpp
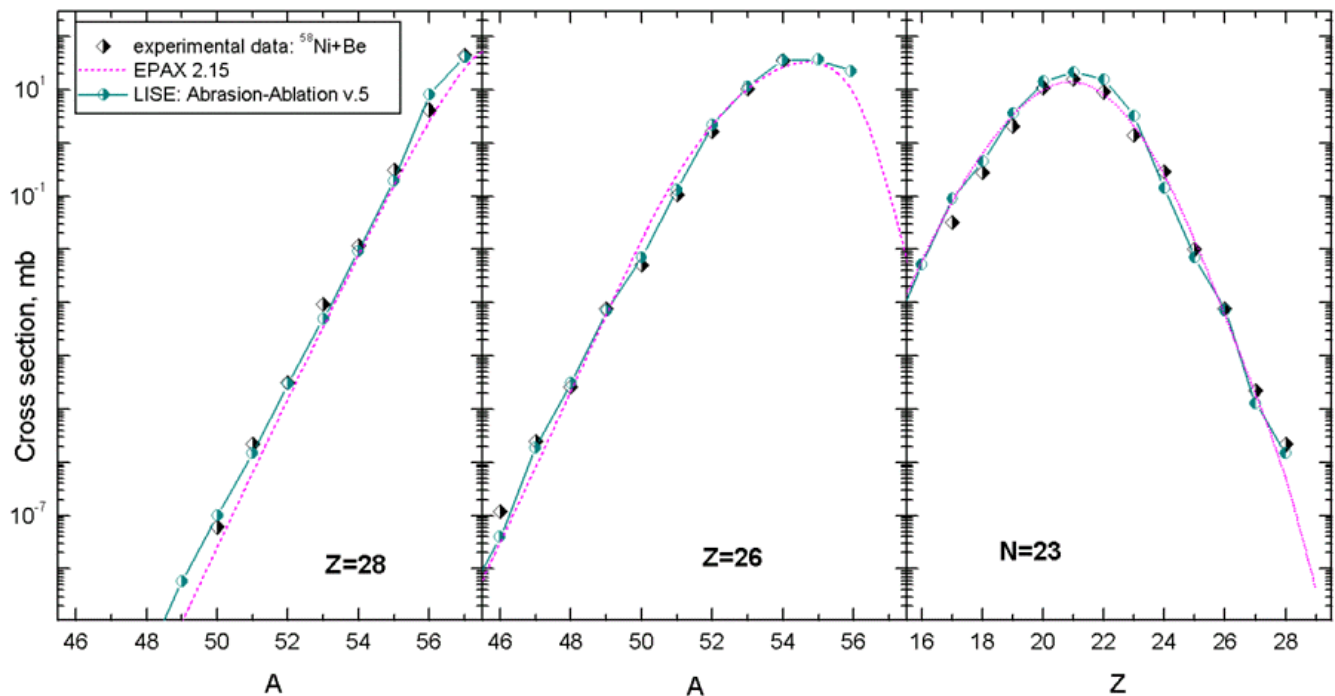

Fig.25. *Experimental [Bla94, Moc03] and calculated (EPAX2.15 & LISE++ Abrasion-Ablation v.5) production cross-section of nickel isotopes (left), iron isotopes (middle plot), and isotones N=23 (right plot) in the reaction $^{58}Ni+Be$ (140MeV/u & 650 MeV/u).*

4.7.2. $^{40}Ar + Be,C$

Experimental cross-sections in the fragmentation of a nucleus ^{40}Ar in different targets [Sym79, Oza00, Not01] were compared with LISE++ AA calculations using the settings obtained in previous chapter for the fragmentation of ^{58}Ni. Experimental [Sym79] and calculated production cross-sections of sodium isotopes with a carbon target are shown Fig.26. Experimental production cross-sections of isobars A=24 and fluorine isotopes in the reaction ^{40}Ar (1GeV/u) + Be [Oza00] and ^{40}Ar (90MeV/u) + Be [Not01] are shown in Fig.27.

Due to the small number of published data points, it is difficult to carry out a comprehensive analysis in the case of the fragmentation of ^{40}Ar. Instead the AA settings obtained for the case of the fragmentation of ^{58}Ni are used and the calculation well describe the experimental data as shown in Fig.26 and Fig.27:
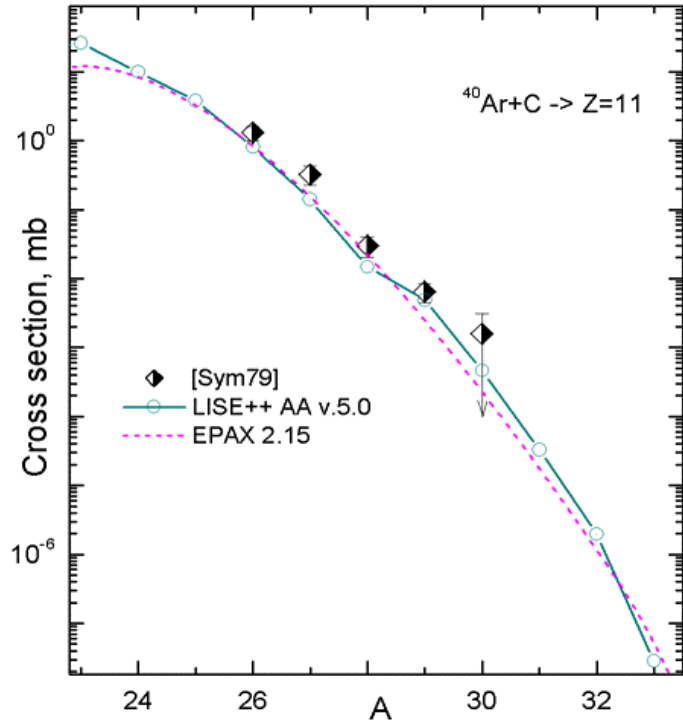

Fig.26. *Experimental [Sym79] and calculated (EPAX2.15 & LISE++ Abrasion-Ablation v.5.) production cross-section of sodium isotopes in the reaction ^{40}Ar+C (205 MeV/u).*

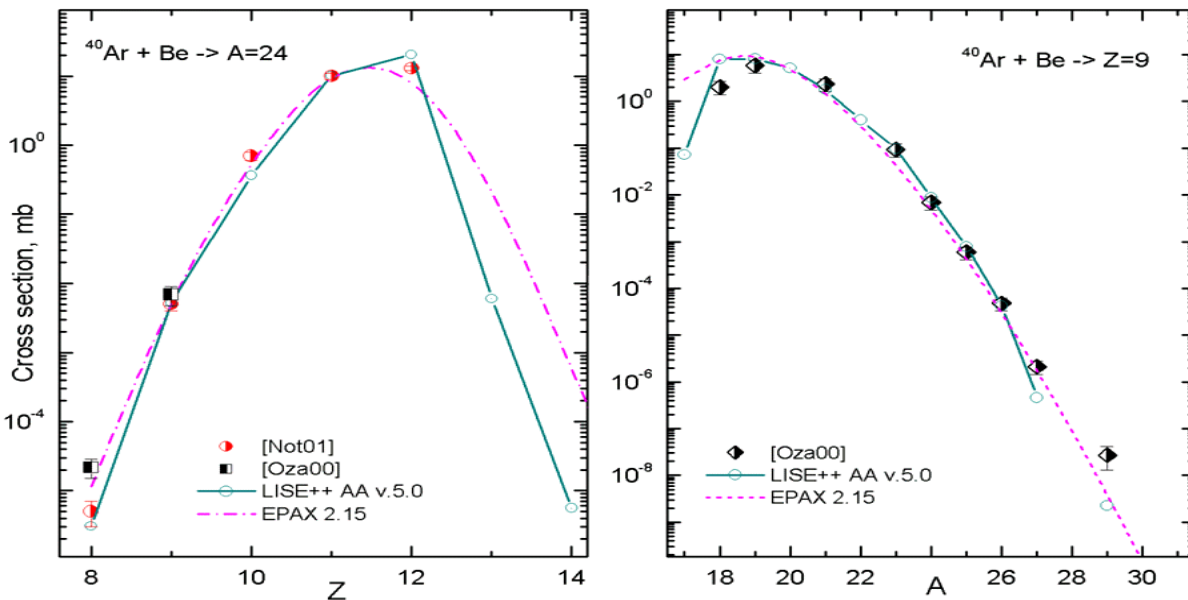| Ex. energy model "C"		Tunl.	shift	modes	Results		
$<E>$	σ	Δ_0	dR		N	$Chi2$	LoD
9.1	5.0	9	5.6	n,p,2p,α	18	25.4	0.3062

Fig.27. *Experimental [Oza00, Not01] and calculated (EPAX2.15 & LISE++ Abrasion-Ablation v.5) production cross-section of isobars A=24 (left plot), and fluorine isotopes (right plot) in the reaction ^{40}Ar+Be.*

4.7.3. Other experimental data

Analysis of some experimental data with AA calculations is still in progress. Experimental data [Tai03] and calculated (EPAX2.15 & LISE++ Abrasion-Ablation v.5) production cross-section of uranium isotopes in the spallation reaction $^{238}U + p$ at 1 AGeV are shown in Fig.28. Plots in Fig.28 demonstrate the influence of "hole energy" (Excitation energy method "B") and "BarFac" values on production cross-sections.
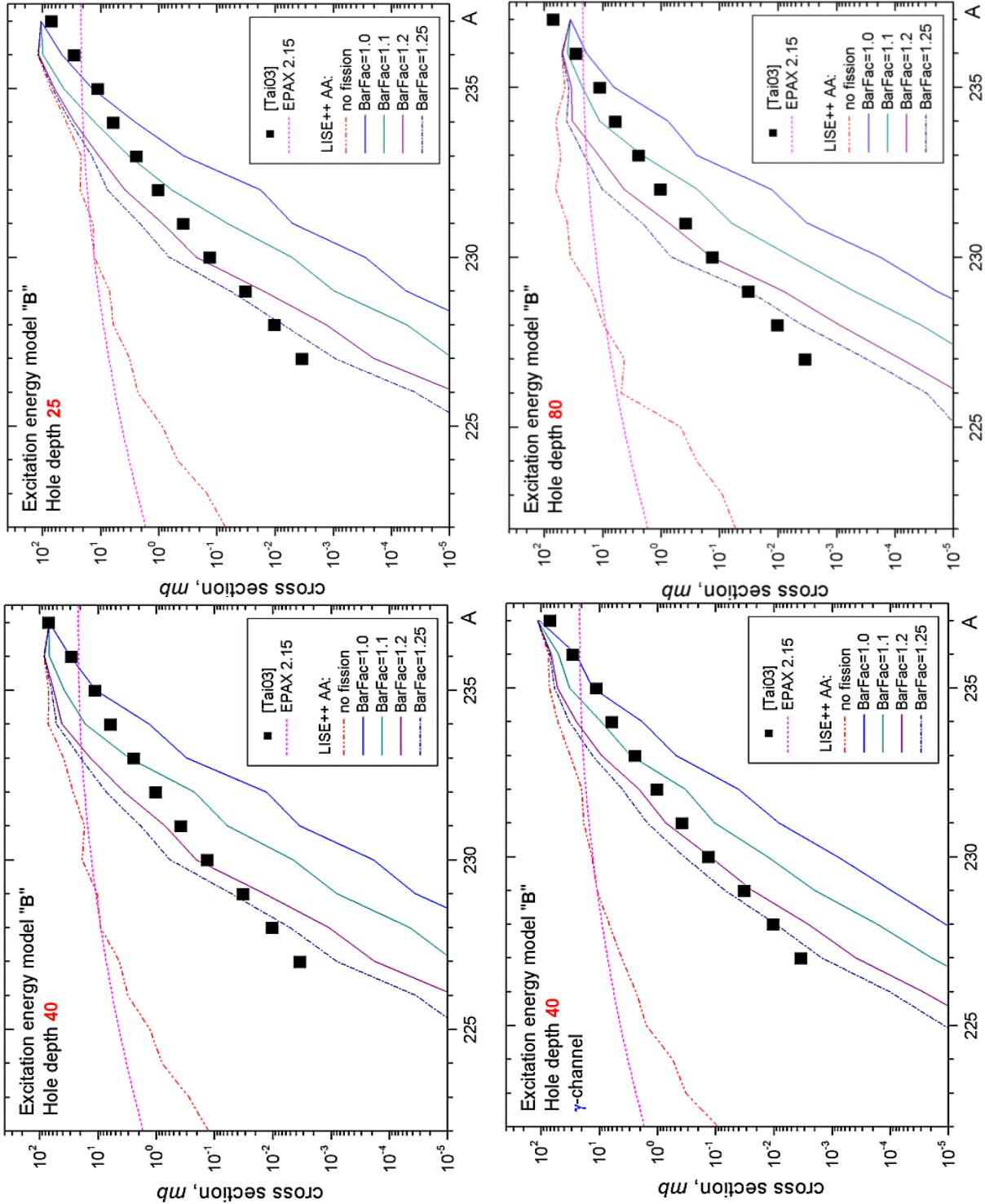

Fig.28. *Experimental [Tai03] and calculated (EPAX2.15 & LISE++ Abrasion-Ablation v.5) production cross-section of uranium isotopes in the spallation reaction $^{238}U + p$ at 1 AGeV.*

The model settings applied for calculations in Fig.28 are listed below:

Ex. energy model "B" *Hole depth*	NP Dimension	Tunl Δ_0	*Shift dR*	Modes	*Density*
25,40,80	64	12	5.7	n,p,α,fission	"C"

From comparison with experimental data it is possible to make conclusion about necessary updating of the fission barrier depending on the angular moment of a nucleus [Jon97].

Some experimental data applied in LISE++ AA analysis can be found in the directory "CrossSections\PublishedData". Most of these data was ported from the personal site of Dr.K.-H.Schmidt (http://www-w2k.gsi.de/kschmidt/data.htm).

Contents of the directory "CrossSections\PublishedData":

```
40Ar_Be_1AGeV.cs          [Oza00]      40Ar_C_240AMeV.cs              [Sym79]
58ni_be_650AMeV.cs        [Bla94]      129Xe_Al_790AMeV.cs            [Rei98]
136Xe_Al_760AMeV.cs       [Zei92]      238U_Pb_1AGeV_fragmentation.cs [Enq99]
238U_p_spallation.cs      [Tai03]      238U_Pb_1AGeV_fission.cs       [Enq99]
      It is planned to add
```

^{208}Pb(1GeV/u)+Cu   [Jon98] ^{36}S(75MeV/u)+Be,Ta   [Tar97]

^{197}Au(950MeV/u)+Be   [Ben99]

4.8. Cross-section & minimum separation energy dependence

A model to relate the experimental cross-sections to neutron separation energies for nuclei far from stability has been proposed by W.A.Friedman and M.B.Tsang [Fri03]. The procedure is based on determining cross section production of nuclei by projectile fragmentation. An Abrasion-Ablation analysis leads to a cross section prediction which is sensitive to the neutron separation energy. LISE++ can be used for such kind of purposes. Moreover it would be desirable to note a number of LISE++ features for this analysis:
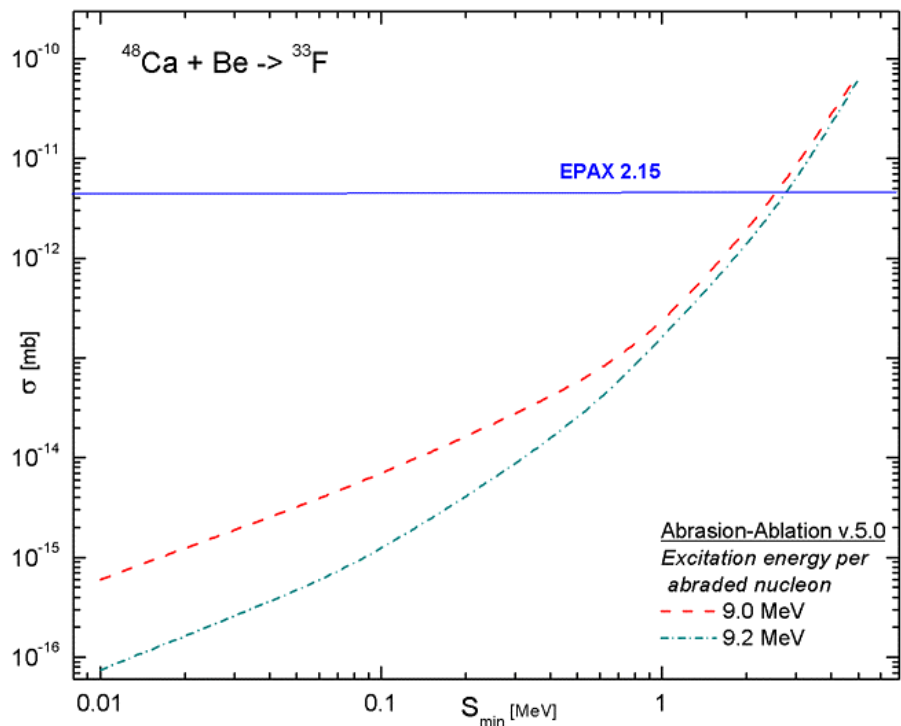

Fig.29. *The predicted cross-sections to produce a nucleus ^{33}F from fragmentation of ^{48}Ca with Be target as a function of the separation energy for ^{33}F nucleus. LISE++ AA settings for the fragmentation of ^{58}Ni with Be target (chapter 4.7.1.) were used to predict cross-sections.*

- Possibility quickly to change a mass excess of a nucleus in the mode "UME file" using the "Databases" dialog (see Fig.2)
- Fast analytical LISE++ Abrasion-Ablation model which is "transparent" for the user.
- The built-in database of measured masses [A&W95].

The predicted cross-sections to produce a nucleus ^{33}F from fragmentation of ^{48}Ca with Be target as a function of the separation energy for ^{33}F nucleus are shown in Fig.29. LISE++ AA settings for the fragmentation of ^{58}Ni with Be target (chapter 4.7.1.) were used to predict cross-sections. The dimension (*NP*) of evaporation distributions was equal to 64, and just one excitation energy region was used in this analysis.

☞ It is necessary to remember that the accuracy of separation energy estimation depends from accuracy of mass measurement of neighbor nuclei used in calculations. It is recommended to use the dimension of evaporation distributions more than 32. For small separation energy the quality of estimation depends very much from LISE++ AA settings (see the energy region 0.01÷0.3 MeV in Fig.29).

4.9. Three step Abrasion-Ablation model

LISE++ Abrasion-Ablation model uses excitation energy models which can not reproduce the following experimental facts:

- Difference between production cross-sections with different target at intermediate energies. Production cross-sections for neutron-rich isotopes for the primary beam at energies 50-200 MeV/u [Tar97] with heavy targets are larger than with light targets.

- Production cross-section dependence from the primary beam energy. With increase of primary beam energy from 50 MeV/u [Tar98] to relativistic energies the neutron-rich production cross-sections decrease.

These observations can be explained by an assumption that the excitation energy in the case of heavy targets and low incident energies is lower than the excitation energy in the case of light targets and high incident energies. The release of excitation energy is larger with an increase of the abrasion time. The abrasion time is proportional to the velocity of fragment and the target size.

In this connection it is suggested to implement three step Abrasion-Ablation in LISE++ where the release of excitation energy is calculated in the intermediate step.

Three step fragmentation model has already been successfully applied to the description of momentum distributions by the Universal parameterization in LISE++ (http://groups.nscl.msu.edu/lise/doc/universal_param.ppt). It was assumed that between abrasion and ablation an intermediate step **"friction"** exists due to kinetic energy loss, exchange of nucleons, and transformation into the internal degrees of freedom. The exponential attenuation is implemented to momentum distribution of fragments due to friction.

5. Other

5.1. Drift block in the Beam analyzer dialog

The possibility to insert a drift block after a dipole has been added in the dialog "Brho analyzer" (see Fig.30,31).
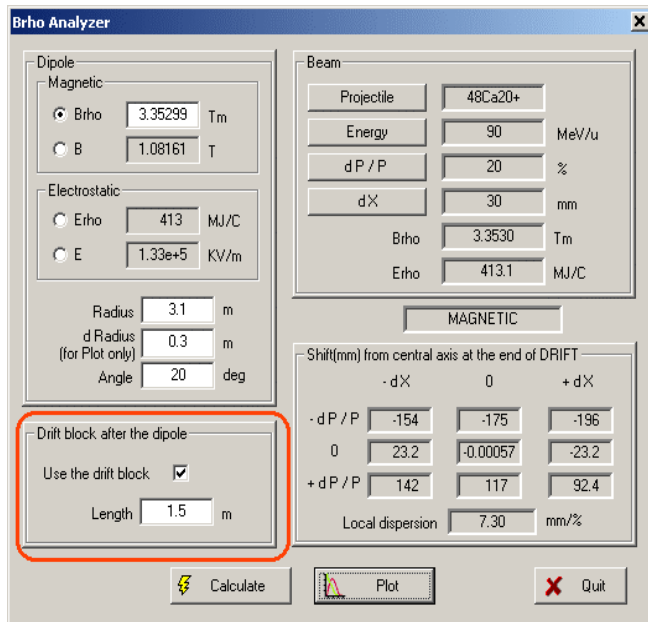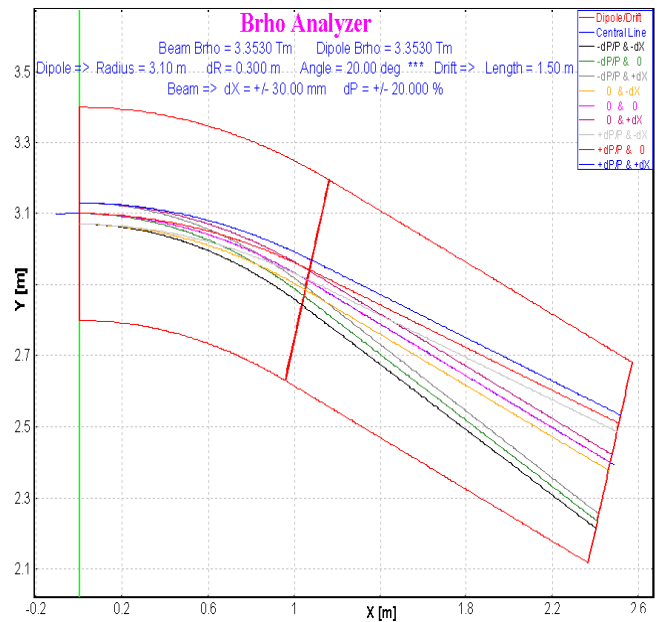

Fig.30. *The "Brho analyzer" dialog*

Fig.31. *"Brho analyzer" plot with the drift option on.*

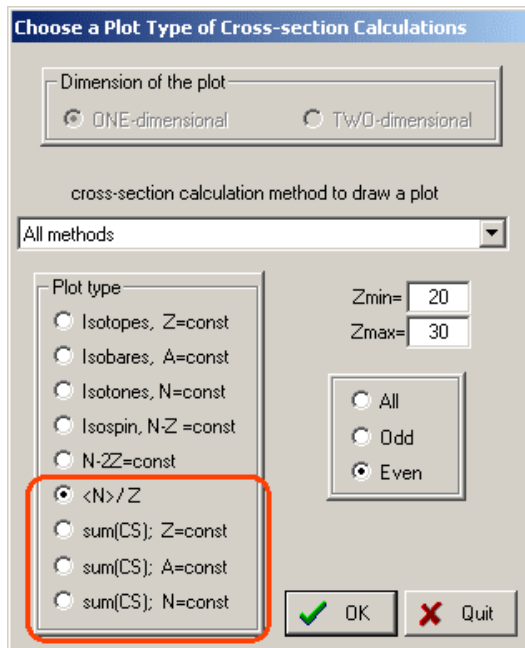## 5.2. New options for cross-section plot

Fig.32. *The cross-sections plot dialog with new options marked by the red rectangle.*
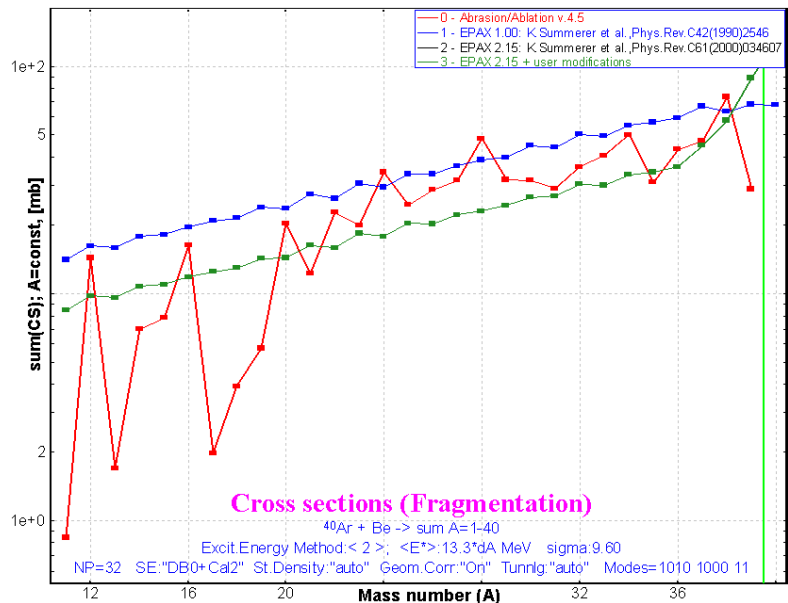

Fig.33. *Example of "sum(CS$_A$)" cross-section plot in the reaction ^{40}Ar+Be.*

Four new options to create cross-section plots have been added in LISE++ (see Fig.32 and Fig.33).

5.3. Writing files from the "Statistics" windows

There are two available "statistics" window in LISE++: the first one is the window of transmissions of fragment when the user clicks the right button of the mouse on an isotope in the table of nuclides, and the second can be created from a one-dimensional plot using the icon ![icon] to show the statistical parameters of distributions. The new version allows users to write the contents of these windows into a file by clicking on the button "File Save".

5.4. PACE4 modifications

5.4.1. Number of cascades

The maximum number of cascades has been increased to 1 million. The previous limit was due to short integers (< 32768) used in the file "*PACE4.evt*". This limit was removed using integer (4 words) format. Increasing the number of cascades increases not only the calculation speed, but also memory allocated for the "event" array (65 MB in the case of one million cascades), as well as the size of the working file (for example, the size of this file is about 635 MB (!!!) in the case of one million cascades for the reaction ^{48}Ca+^{124}Sn with a primary beam energy at $E_{lab} = 200$ MeV). If the fusion cross-section is 1 barn, using 1 million of cascades it is possible to reach the 1 nb limit.

Fig.34. *PACE4 calculations (1 million of cascades) for the reaction ^{48}Ca(200MeV)+^{124}Sn.*

5.4.2. BarFac modifications

The "*BarFac*" parameter determinates the fission barrier characteristics and can be modified in the first dialog of the code PACE4. The program assumes the A.J.Sierk modified rotating liquid drop barrier if the atomic number of the compound is one of these values: 68,76,84. For other atomic number of the compound the code uses a rotating liquid drop fission barrier from the work [Coh63].

- If *BarFac* is positive the value will be taken as a spin for the desired zero spin fission barrier.
- If *BarFac* is negative, its absolute value will be taken as a factor to the fission barrier.

It is planned to implement in the code PACE4 (as well as in LISE++) a new model of fission barrier which allows to calculate more correctly the fission barrier, in particular for compound nuclei heavier than uranium.

5.4.3. Cross-section file

The format of PACE4 cross-section files has been changed. The new extension of PACE4 is "*.cs4*", whereas for all User CSF the extension is "*.cs*". PACE4 CSF is saved by default in the directory "LISE\CrossSections". In the previous versions cross-sections were saved in the same directory where the PACE4 input file was located.
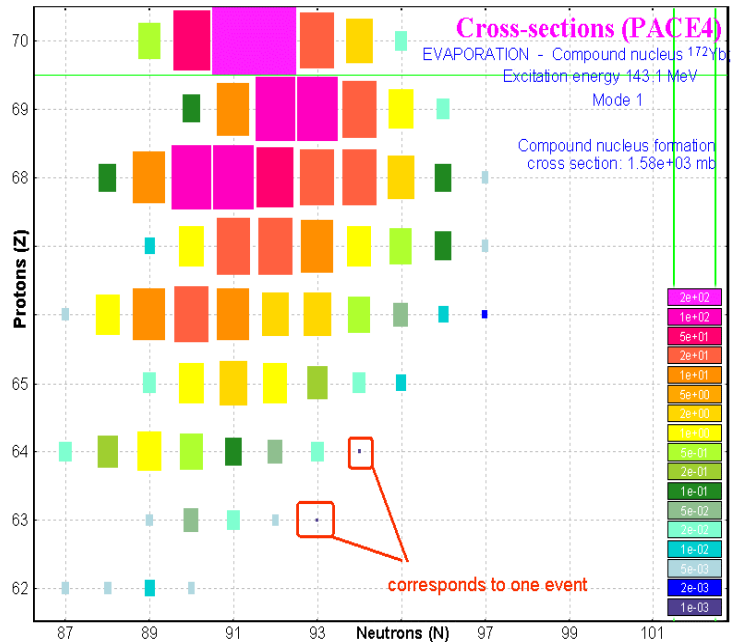
5.5. Secondary reactions (in target) corrections

The procedure to calculate the contribution from secondary reactions in the target into the final counting rate of fragments has been revised. As marked earlier in the LISE documentation the contribution of secondary reactions is reasonable for energies above 500 MeV/u. These estimations were made for ^{28}O and ^{29}F. However, for more neutron-rich isotopes, it is possible to get considerable fields from secondary reactions at much lower energies as for example 140 MeV per nucleon shown in Fig.35. For example, a factor 2 can be gained for the particle bound ^{31}F isotope (see Fig.35).
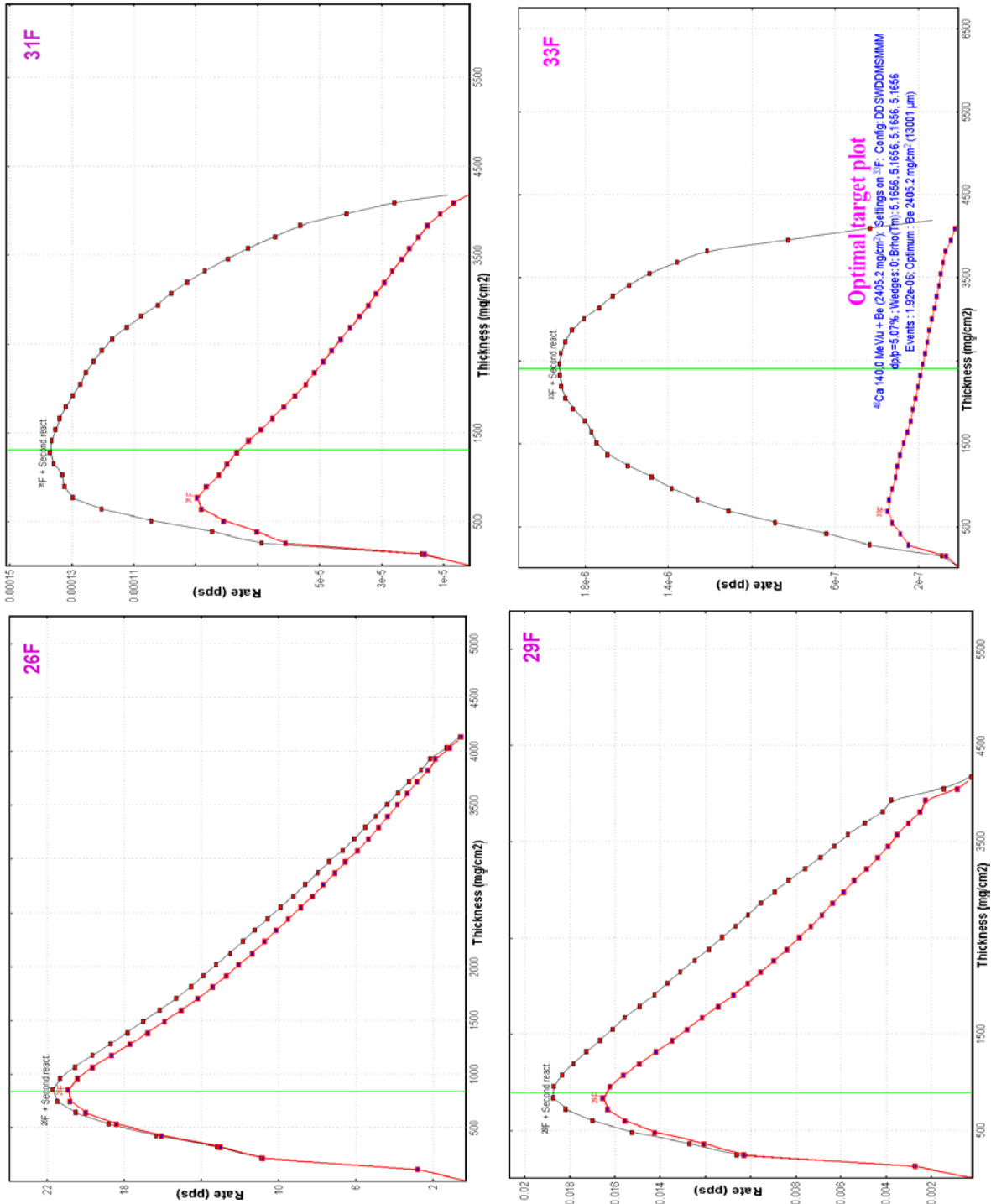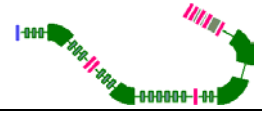

Fig.35. *Optimal target thickness calculation plots for the fluorine neutron-rich isotopes $^{26,29,31,33}F$ in the reaction $^{48}Ca(140MeV/u, 1 pnA)+Be$ using the A1900 fragment separator. The black top curves represent the rates of fragment of interest taking into account secondary reactions in the target, the red bottom curves without contribution of secondary reactions. Calculations were done using the EPAX 2.15 parameterization.*

5.6. Configuration files

RIKEN	RIPS.lcn (T.Kubo)	corrected
NSCL	A1900-N4-gas_cell.lcn (D.Morrissey)	corrected
	A1900 – 4 dipoles.lcn	The same as A1900_PAC27.lcn
	BL+S800_d0.lcn (former S800_d0.lcn) BL+S800_dm.lcn (former S800_dm.lcn)	
	New configuration: S800.lcn	

5.7. Bug report

Two-dimensional "ellipse" plot L.Sobotka (WU)	Shift of fragment peak position in the case of "ellipse" drawing mode for two-dimensional plots. *Fixed.*
LISE's file reading K.Starosta (NSCL)	Wrong reading of slit parameters if the slit had different left and right positions. *Fixed.*
Fusion cross-section calculations in versions 6.3.15-21 P.Sugathan (NSC, New Delhi)	The code crashed in fusion-residue mode in the process of residue transmission calculation. It happened due to a recent change of reaction order. *Fixed.*
Slit & Acceptance settings dialog M.Hausmann (LANL)	The code didn't restore previous settings and kept changed values then the button "Cancel" was pressed. *Fixed.*
Fragment energy after reaction and Width of momentum distributions at relativistic energies H.Weik (GSI)	This is a serious problem for relativistic energies, which was not taken into account before for intermediate energies. Calculated fragment momentum distribution is narrower than actually should be. *Fixed.* *In connection to this bug all calculations done by the previous versions will be repeated at loading.*
Secondary reactions (in target) corrections	See chapter 5.5. Secondary reactions (in target) corrections.

All user's remarks, wishes are welcome!

Acknowledgements

References:

[A&W95]   G.Audi and A.H.Wapstra, Atom.Data and Nucl.Data Tables (1995) 1.

[Ben98]   J.Benlliure et al., Eur.Phys.J. A 2 (1998) 193.

[Ben99]   J.Benlliure et al., Nucl.Phys.A 660 (1999) 87.

[Bla94]   B.Blank et al., Phys.Rev.C 50 (1994) 2398.

[Coh63]   S.Cohen and W.J.Swiatecki, Ann. Phys. 22 (1963) 406.

[Enq99]   T. Enqvist et al., Nucl. Phys. A 658 (1999) 47-66.

[Fri03]   W.A.Friedman and M.B.Tsang, Phys.Rev.C67 (2003) 051601.

[Ign67]   A.V.Ignatyuk et al., Yad.Fiz. 21 (1975) 485.

[Ilj92]   A.S.Iljinov et al., Nucl. Phys. A543 (1992) 517-557.

[Jon97]   M.de Jong et al., Nucl.Phys.A613 (1997) 435.

[Jon98]   M.de Jong et al., Nucl.Phys.A628 (1998) 479.

[Moc03]   M.Mocko et al. to be printed.

[Not01]   M.Notani, PhD thesis, University of Tokyo (2001).

[Oga98]   Yu.Ts.Oganessian, et al., Proceedings of IV Int. Conf. on Dynamical Aspects of Nuclear Fission, 19–23 Oct1998, Casta-Papiernicka, Slovak Republic, World Scientic, Singapore, 2000, p. 334.

[Oza00]   A.Ozawa et al., Nucl.Phys. A673 (2000) 411.

[Rei98]   J.Reinhold et al., Phys.Rev.C58 (1998) 247.

[Sch02]   K.-H.Schmidt et al., Nuclear Physics A 710 (2002) 157-179.

[Sym79]   T.J.M.Symons et al.,Phys.Rev. C42 (1979) 40.

[Tai03]   J.Taïeb et al, Nucl.Phys. A724 (2003) 413.

[Tar97]   O.Tarasov et al., Phys.Lett. B407 (1997) 64.

[Tar98]   O.Tarasov et al., Nucl.Phys. A629 (1998) 605.

[Sar00]   F.Sarazin et al., PRL 84 (2000) 5062.

[Zei92]   K.Zeitelhack, PhD thesis, Universität München, Physik Department E12, 1992.